Model Calculation of Field Enhancement Factor of CNTs having Conical tip taking into account the Shielding Effect.

A Dissertation submitted towards the partial fulfillment of the requirement for the award of degree of

Master of Technology in

Nano Science and Technology

Submitted by

Smriti Shit

2K14/NST/18

Under the Supervision of

Prof. S.C. Sharma (HOD, Applied Physics)

Department of Applied Physics,

Delhi Technological University

(Formerly Delhi College of Engineering)
Delhi-110042

JUNE 2016

DELHI TECHNOLOGICAL UNIVERSITY

Established by Govt. of Delhi vide Act 6 of 2006

(Formerly Delhi College of Engineering)

SHAHBAD, DAULATPUR, BAWANA ROAD

DELHI-110042

CERTIFICATE

This is to certify that work which is being presented in the dissertation entitled **Model Calculation of Field Enhancement Factor of CNTs having Conical tip taking into account the Shielding Effect** is the authentic work of **Smriti Shit** under my guidance and supervision in the partial fulfilment of requirement towards the of **Master of Technology in Nano Science and Technology**, run by Department of Applied Physics in Delhi Technological University during the year 2014-2016.

As per candidate declaration this work has not been submitted elsewhere for the award of any degree/diploma.

Prof. S. C. Sharma
Supervisor
H.O.D., Applied Physics
Delhi Technological University, Delhi

DECLARATION

I, hereby, declare that all the information in this document has been obtained and presented in accordance with the academic rules and ethical conduct. This report is my own, unaided work. I have fully cited and referenced all material and results that are not original to this work. It is being submitted for the degree of Master of Technology in Nano Science and Technology at the Delhi Technological University. It has not been submitted before for any degree/diploma or examination in any other university.

Signature:
Name: Smriti Shit

ACKNOWLEDGEMENT

I take this opportunity as a privilege to thank all individuals without whose support and guidance I could not have completed my project successfully in this stipulated period of time.

First and foremost I would like to express my deepest gratitude to my supervisor **Prof. S.C. Sharma**, HOD, Applied Physics, for his invaluable support, guidance, motivation and encouragement throughout the period of this work.

I am also thankful to **Mr. Ravi Gupta, Ms Neha Gupta** and **Ms Aarti Tewari (Research scholars)** for their valuable support and guidance in carrying out this project.

I am deeply grateful to **Dr. M.S.Mehata, Assistant Prof** (Branch coordinator, NST) for his support and encouragement in carrying out this project.

I also wish to express my heartfelt thanks to staff at Department of Applied Physics of Delhi Technological University for their goodwill and support that helped me a lot in successful completion of this project.

.

Smriti Shit
2K14/NST/18

ABSTRACT

This thesis presents a method to compute the field enhancement factor of individual CNT with conical tip and the field enhancement of the same CNT when placed in a cluster of CNTs under any position distribution using mirror method and taking into account the image charge. When the CNT is present in a group of CNTs the shielding effect comes into picture and this shielding effect depends upon length and the spacing between the CNTs.We have derived expressions for field enhancement factor with and without taking into account the screening effect. The variation of the field enhancement factor with the sharpness of the tip is shown. Later we have shown the comparisons with the experimental and theoretical results of the CNTs having hemispherical tip and it was found that the field enhancement factor of the CNTs having conical tip is higher than that of the hemispherical tip, thus offering a better field emission.

TABLE OF CONTENTS

LIST OF FIGURES

LIST OF TABLES

LIST OF SYMBOLS

V(r)	Potential energy
σ	Surface Charge density
r	Distance from the center of the base of the conical tip of the CNT
h′	Length of CNT
H	Height of the conical tip
R	Radius of the base of the conical tip CNT
β	Field enhancement factor
ε_0	Permittivity in free space
q	Electric charge
h	Planck's constant

CHAPTER 1: INTRODUCTION

1.1 BACKGROUND BEHIND THE DISCOVERY OF CNTs

Earlier it was thought that the pure solid carbon exists in only two different physical form, graphite and diamond. These two well-known forms of elemental carbon are called allotropes. In 1985 discovery of a new allotropic form of elemental carbon took place which created excitement among the scientist. Harold W. Kroto of the University of Sussex in England joined Robert F. Curl and Richard E. Smalley at Rice University in Texas in Smalley's lab to study the products of carbon vaporization where they fired high energy laser beam at the graphite surface and to carry the fragments to the mass spectrometer used a stream of Helium gas. These fragments interacted among themselves depending on the pressure of helium gas on their way to the mass spectrometer leading to the formation of most stable form carbon atom cluster i.e C_{60}which is a sixty carbon atom cage arranged in the form of a ball. Later it is known as 'buckminsterfullerene' or 'buckyball' named after famous architect, Buckminster Fuller. With this discovery of an infinite class of molecules took place (Fullerenes)

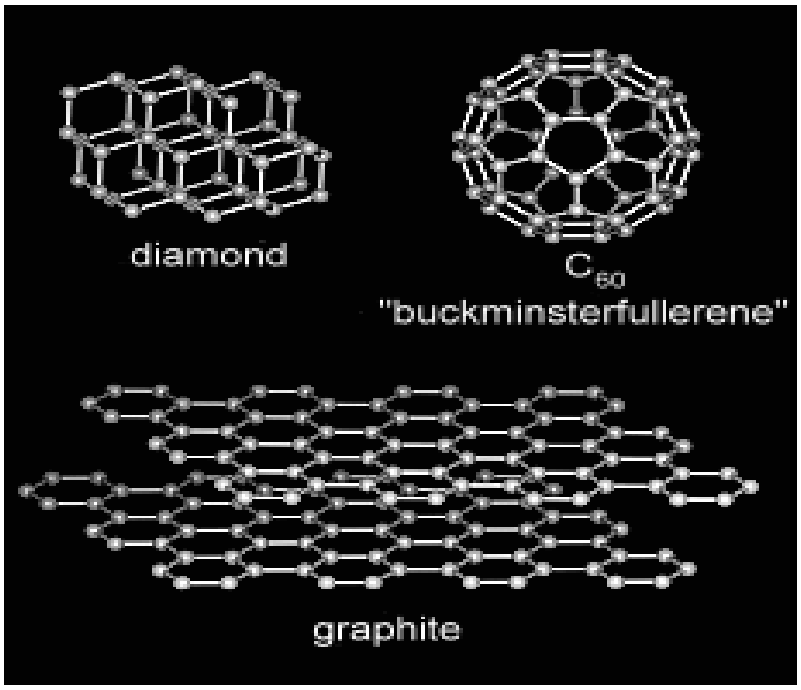

Fig 1.1 Arrangement of Carbon atom in Diamond, Graphite and Buckminsterfullerene

1.2 DISCOVERY OF CNTs

Though Carbon nanotubes had been discovered 30 years earlier, but it had not been taken into account since it was not verified. In 1991, multiwall nanotubes were observed in carbon arc discharge by Sumio Iijimia. Two years later single-wall nanotubes were observed by Sumio Iijimia and Donald Bethune independently.

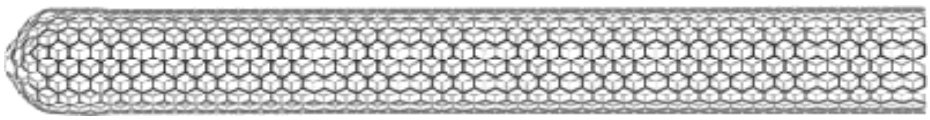

Fig1.2 Carbon Nanotube

1.3 CLASSIFICATION AND STRUCTURE OF CNTs

Carbon nanotubes (CNTs) are seamless hollow elongated cylinders of carbon atoms consisting of one or more than one hexagonal graphene layers rolled into a tube. Theoretically when a graphene sheet is rolled up to carbon nanotube re hybridization occurs. The orbital structure of carbon changes due to change in bond length and bond angle. Bond length between the carbon atom decreases and also the σ- and π- orbitals are not perpendicular to each other. A mixed state of σ- and π- orbitals is introduced due to the curvature.

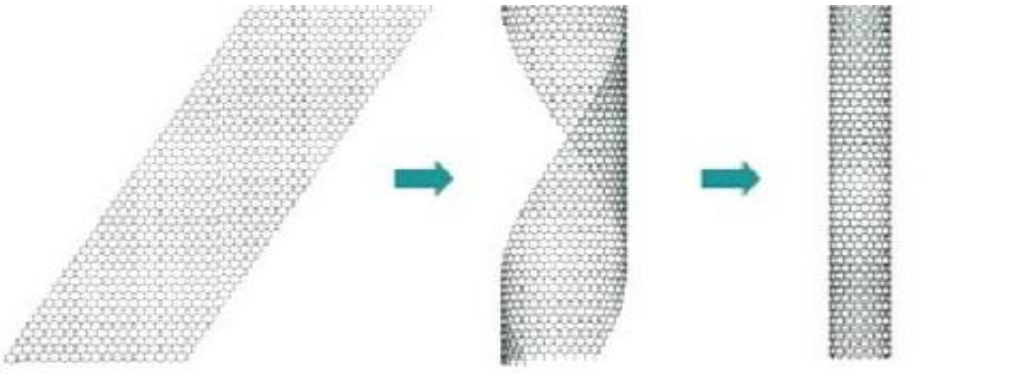

Fig1.3 (i) Graphene sheet rolled to form Carbon nanotube

Carbon nanotubes can be broadly divided into

(i) Single Walled Nanotubes (SWNTs)

(ii) Multi walled Nanotubes (MWNTs)

Single Walled Nanotubes (SWNTs) and Multi Walled Nanotubes differs in the graphene layers arrangement. SWNTs are made up of single graphene cylinder whereas MWNTs are made up of coaxial single walled nanotubes with a inter wall separation of 0.342nm which is equal to interlayer separation of graphite sheets.

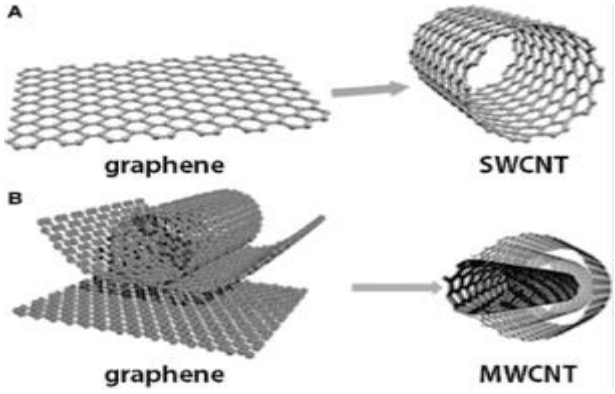

Fig 1.3 (ii) Graphene layer rolled to form SWNT and MWNT

Structure of Carbon nanotubes depend on the orientation of the hexagon in the honeycomb lattice relative to the axis of the nanotube. The vector which defines these structures is called chiral vector.

$C_h = n\widehat{a_1} + m\widehat{a_2}$

where n and m ($0 \leq |m| \leq n$) are integers and a_1 and a_2 are real space unit vectors. The chiral vector also introduces an angle called chiral angle"θ" which is the angle between the chiral vector C_h and a_1 and it lie between 0° to 30° due to the hexagonal symmetry of the honeycomb lattice. Chiral angle also express the spiral symmetry. It can be also defined as the tilt angle of the hexagon w.r.t the the direction of the nanotube axis. Thus the chiral angle θ is expressed as

$$\cos\theta = \frac{2n + m}{2\sqrt{n^2 + m^2 + nm}}$$

The diameter of the CNT "d" can be expressed as d= $\frac{L}{\pi}$, L is the circumferential length of the carbon nanotube.

$L = |C_h| = a\sqrt{n^2 + m^2 + nm}$. It should be noted that a_1 and a_2 are not orthogonal to each other and their inner product gives us

$a_1.a_1 = a_2.a_2 = a^2$ and $a_1.a_2 = \frac{a^2}{2}$

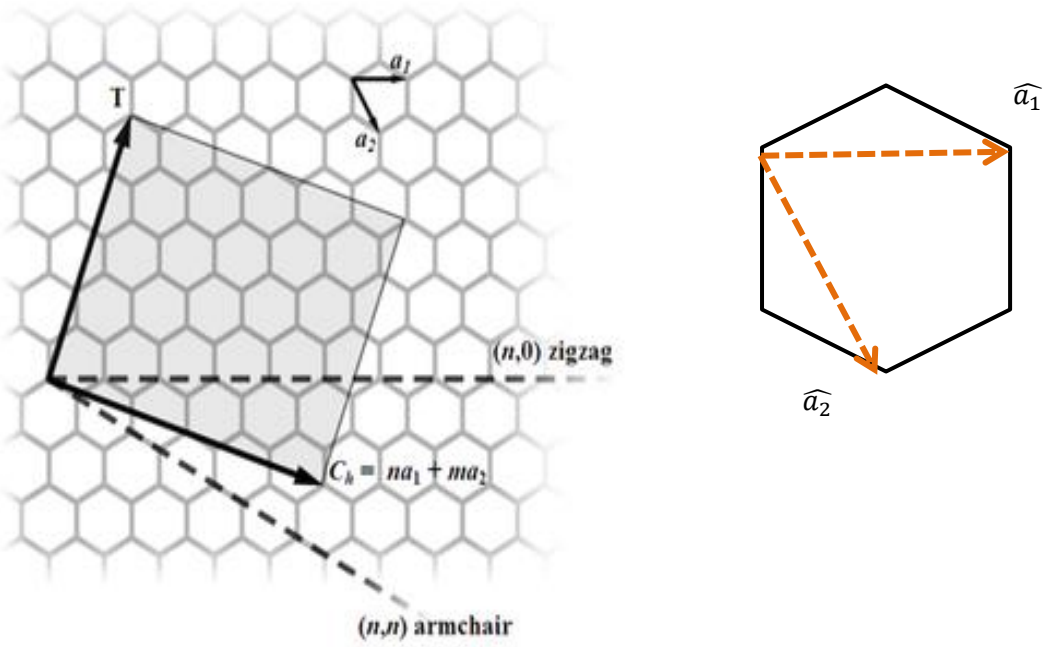

Fig1.3 (iii) The honeycomb lattice of a nanotube with the chiral vector C_h and the translational vector T

Translational vector can be defined as the unit vector of 1D carbon nanotube which is parallel to the nanotube axis and is normal to chiral vector C_h as shown in the unrolled honeycomb lattice of the nanotube.

On the basis of the chiral vector and the chiral angle carbon nanotubes can be classified into three different groups.

1. Armchair ((n,n),$\theta = 30°$, shape of the cross section- cis type)
2. Zig Zag ((n,0),$\theta = 0°$, shape of the cross section- trans type)
3. Chiral ((n,m),$0° \leq |\theta| \leq 30°$, shape of the cross section-mixture of cis and trans)

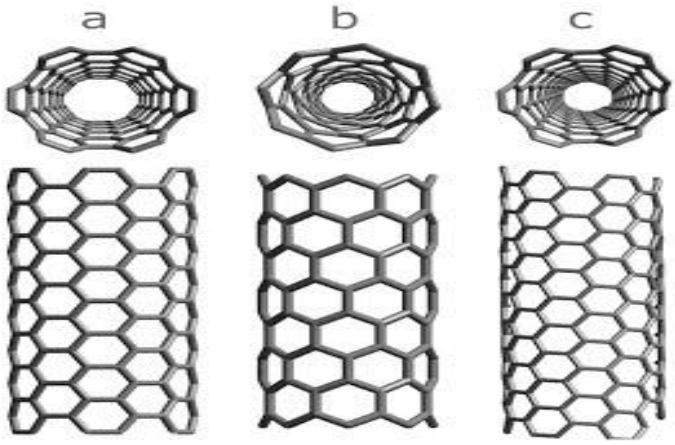

Fig1.3 (iv) Schematic model of (a) an arm chair nanotube (b) a zig- zag nanotube

(c) a chiral nanotube

The Armchair and the Zig Zag nanotubes shares a high degree of symmetry while the Chiral nanotube structure can be available in two mirror image form.

1.4 PROPERTIES OF CARBON NANOTUBE

The extraordinary properties of CNTs are due to the unique structural feature of CNTs, amongst which are

(i) Six carbon atoms forming a hexagon and are covalently bonded through sp2 hybridized orbitals leading to the formation of planar structure with six delocalized π electrons on the both side of the plane.

(ii) Replication of six membered ring leads to the formation of 2D sheet called **graphene sheet**. CNTs are formed by rolling the graphene sheet, thus the graphene sheet helps in movement of delocalised π electron across the sheet. Since graphene sheet is only one atom in thickness whichalso facilitates all the carbon atoms exposed to the surroundings.

(iii) CNT has a **tubular** structure at the atomic level which confined the movement of delocalised electron along the cross section and their mobility is along the length of the tube, hence making CNT a 1D nanostructure.

(iv) There are two sources of **anisotropy** (property of being directionally dependant) in CNTs

(a) 2D confinement due to the high aspect ratio

(b) Chirality which arises due to the orientation in which the graphene sheet is rolled with respect to the hexagonal structure.

(v) CNTs may be **Single walled** or **Multi walled** which means their diameter varies according to the number of co axial cylinder present in it.

(vi) The ends of the nanotube may be **open ended** or **close ended** and these ends are **highly reactive** due to imbalance in the bond structure.

(vii) The surface of the nanotube has delocalised π electron which creates a Van der waals force at the point of contact and causes **inter tube attraction**

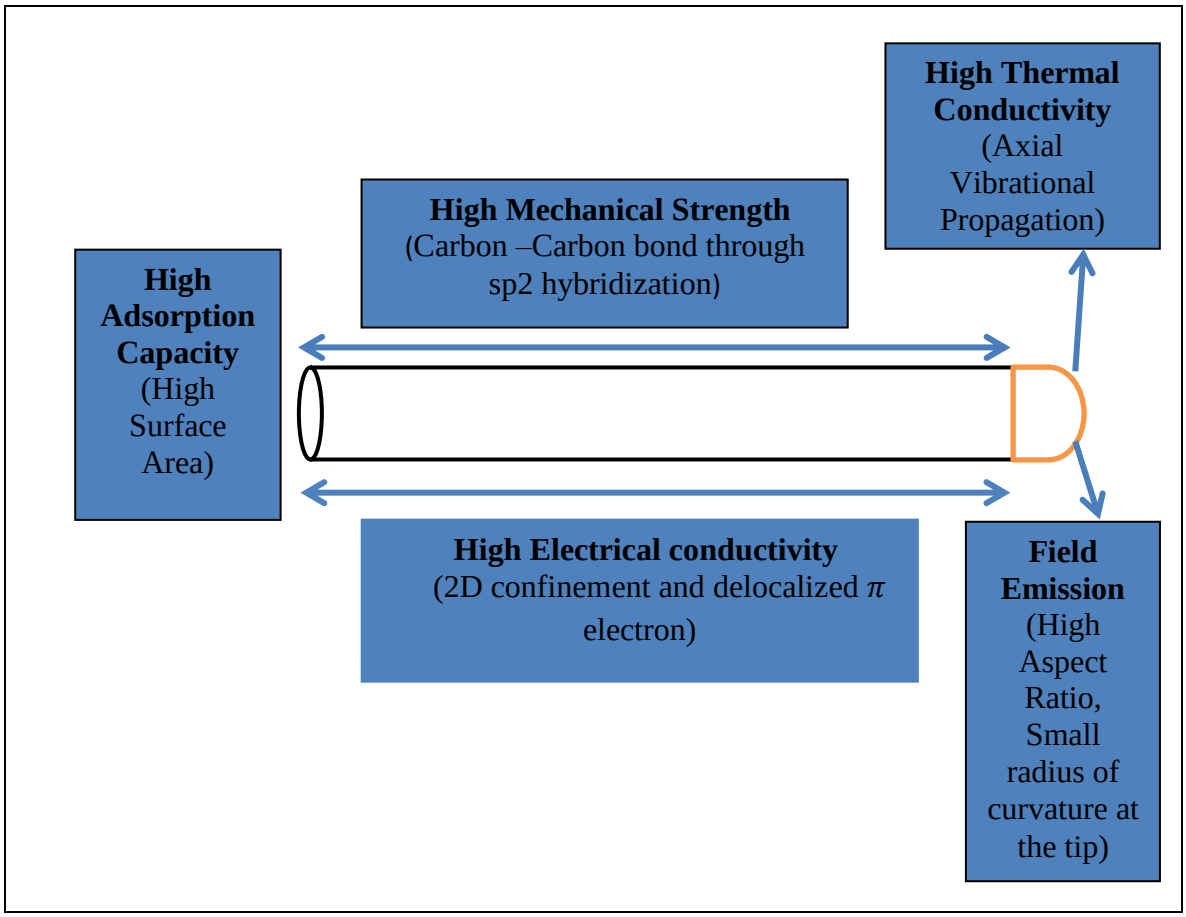

Fig 1.4 Properties of Carbon Nanotubes

Carbon nanotubes show many extraordinary properties which endow them a special place in the world of nanomaterial. Their extraordinary properties empower researcher and scientists to consider using them in several fields. Some of the extraordinary properties are listed below:

(i) Mechanical Strength

(ii) Electrical Conductivity

(iii) Thermal Conductivity

(iv) Adsorption Capacity

(v) Field Emission

1.4.1 Mechanical Properties

Wong *et al*. [30] also determine the elasticity; toughness and strength of SWNT.Carbon nanotubes are extremely strong along their axis and have very high Young's Modulus along the axial direction. So far they are strongest and stiffest material known. This strength arises due to the strong sp2 hybridized Carbon-Carbon covalent bonding. A single nanotube is 10 or 100 times stronger than steel per unit weight. The Young Modulus of a CNT can go up to 1000GPa which is almost 5 times higher than steel and the Tensile strength i.e. the breaking strain of nanotube be as high as 63 GPa which 50 times higher than steel.

The theoretical predictions of CNTs having high Young's moduli along with the extraordinary flexibility and resilience are confirmed by various techniques like high-resolution transmission electron microscopy (HRTEM) and atomic force microscopy (AFM).Along with the most notable achievement and experiments in past years in the determining the mechanical properties of CNTs, a qualitative relation between the Young modulus and the amount of disorder in atomic structure of walls and how the mechanical properties of CNTs will be improved by composites are shown by **Salvetat** *et al.* [31].Various experimental observations were made by various scientists considering CNT as a structural member(e.g bar, shell, beam). **Lourie and Wagner** *et al.* [32] considered bar model and used micro-Raman spectroscopy to determine Young's Modulus**. Yu** *et al.* [33] performed direct tensile test on SWNT and **Yu and Lourie** *et al.* [34] on MWNT.

1.4.2 Electrical Properties

A SWNT is formed by folding a graphene sheet into a cylindrical form. Graphene is 0 gap semiconductor or metal because the DOS is 0 at the Fermi level and it is imparted to the nanotube. We can say that chirality and the diameter of the CNT determines whether it will behave as metal or semiconductor. It was predicted through the tight binding electronic calculation that the relationship between the coefficients (n and m) of the translational vector $C_h = na_1 + ma_2$ which connects two crystallographically equivalent sites, determines the

conducting properties. The zig-zag (n, 0) tubes have Fermi level crossing at the centre of the Brillouin zone (k = 0) and therefore can be metallic or semiconducting whereas arm-chair (n, n) tubes, the level crossings are at $k = \frac{2\pi}{3a_0}$ and they are always metallic. **Ajayan** *et al*. [36] has discussed that when SWNTs are formed in large amount, maximum portion of the tubes have armchair (or close to armchair) arrangement independent of the conditions used in the synthesis. One of the interesting thing which we encounter in a CNTs are their electrical resistance varies if any other molecule get attached to the carbon atom.

For MWNTs, the current flow only occurs through the outer most nanotube cylinder. The adjacent coaxial cylinders has mutual interaction between themselves which might be very small, but cannot be neglected completely, and which makes for a richer band structure in contrast to SWNTs and comparable to graphite as discussed by **Bandaru** *et al.* [37].

1.4.3 Thermal Properties

Specific heat: Phonons are the dominant excitation in 3D graphite, 2D graphene and the nanotubes hence the phonon specific heat C_{ph} dominates C(T)(specific heat) at most temperatures. The thermal properties of CNTs shows behaviours related to their graphitic nature, unique structure and size. CNTs show similar specific heat capacity as that of 2D graphene sheet at higher temperature. At low temperature the specific heat resemble that of 3D graphite. In SWNT ropes inter-tube coupling and interlayer coupling in MWNTs causes this type resemblance**.** A variation of the calculated specific heat from the known phonon band structure of graphene and graphite, from the predicted band structure of an isolated SWNT, and from the predicted band structure of a SWNT bundle with temperature is shown by **Hone** *et al.* [38]. At temperatures above ∼100 K, the specific heat of all four materials is similar but at lower temperatures, there is a substantial diversion in specific heats. The isolated graphene sheet shows the largest specific heat and is more or less linear with T. At the lowest temperatures, the isolated nanotube C(T) is linear with T. 1-D quantization of the phonon band structure occurs as the measured specific heat of SWNTs matches the calculations based on the phonon band structure of isolated nanotubes as discussed by **Hone** *et al.* [38].

Thermal conductivity: Berber *et al*. [39] have calculated the phonon thermal conductivity of isolated nanotubes and have predicted the thermal conductivity of 6600 W/m K for individual nanotubes at room-temperature. Measurements shows for bulk samples of single-

walled nanotubes thermal conductivity over 200 W/m K, and for individual multi walled nanotubes over 3000 W/m K.

1.4.4 Optical Properties

SWNTs have inherent near infra-red photoluminescence and Raman scattering properties. **Kataura** *et al.* [40] measured the optical absorption spectrum and the absorption peaks which are due to the optical transition between the image mirror spikes to semiconducting and metallic tubes. Distribution of diameter in SWNTs can be estimated from the absorption spectrum. The ratio of mixture of the metallic and semiconducting tubes can also be determined from the intensity ratio between absorption peaks due to metallic and semiconducting phase.

1.4.5 Field Emission Properties

Carbon nanotubes have strong potential of application to electron emission sources because they have the capability to emit high currents (up to 1A/cm^2) at low fields (5V/mm) which is demonstrated by **Bonard** and **Nilsson** *et al.* [41].Properties like high aspect ratio, small radius of curvature at their tips, high chemical stability and mechanical strength make CNTs competent enough to be used as field emitters.

Since Carbon nanotubes are formed by rolling the graphene sheet and each carbon is bonded to the other carbon atoms by sp2 hybridization forming a covalent bond, the activation energy for field migration is very high compared to other field emitters like tungsten which helps the tip to withstand very high electric field required for field emission. The arrangement of the Carbon atoms decides the CNT to be metallic or semiconducting **Rinzler** discussed about the high aspect ratio, a small radius of curvature of the cap and good conductance of CNTs compared to other field emitters.

Saito *et al.* [42] have studied that CNTs are chemically inert, and react under extreme conditions or at high temperature with oxygen or hydrogen

The sputter coefficients of carbon are quite low (**Paulmier** *et al*. 2001). Since an electron source is usually bombarded by positive ions therefore it's advantageous to have low sputter coefficient.

In 1995, **De Heer**, **Andre Chatelain** and **Daniel Urgate** first proposed the use of nanotubes as Field Emitter

Field emission:

The extraction of electron from the surface of the solid by overcoming the potential barrier with the application of electric field and voltage is known as **Field Emission**. **Work function** and **the local electric** field near the surface are the two factors on which the emitted current varies.

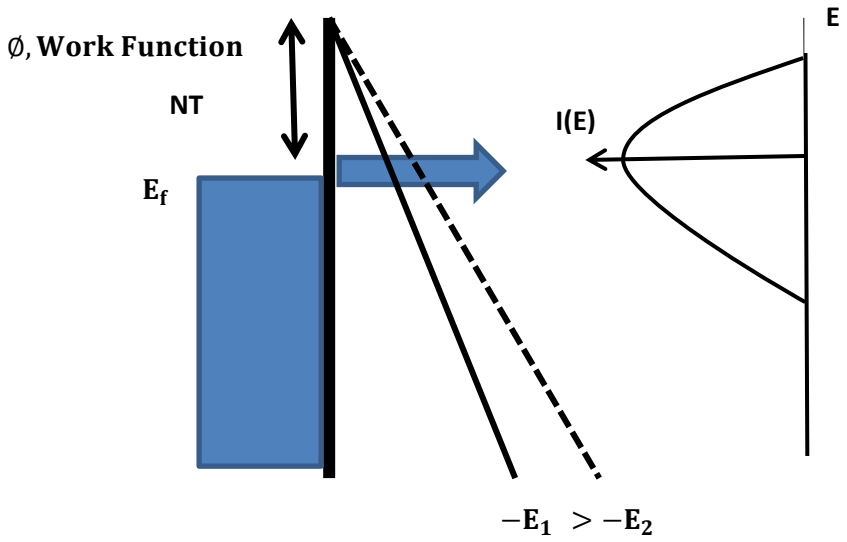

Fig1.4.5 (i) Field Emission Model for a metallic emitter showing the potential barrier and the corresponding energy distribution (Energy on the vertical axis and the current on the horizontal logarithmic axis)

Fowler-Nordheim Equation:

The theory behind the field emission in bulk materials was first proposed by Ralph H. Fowler and Lothar Wolfgang Nordheim. A family of approximated equations are named after them. When a very high electric field is applied at the surface of an electron conductor a wave-mechanical tunnelling of electrons occurs through a rounded triangular barrier. This is known as **Fowler-Nordheim tunnelling**. According to **Fowler–Nordheim model** the emitted current is exponentially dependent on the local electric field, E and the work function ∅.

At low temperature that is T→ 0 the classical expression of **F-N current density** is expressed as,

$$J = AE^2 e^{-\left(\frac{B}{E}\right)},$$

$A = \frac{q^2}{8\pi h\emptyset}$ and $B = -\frac{4}{3}\sqrt{\frac{8\pi^2 m}{h^2}}\frac{(q\emptyset)^{3/2}}{\emptyset}$,

where,

J = Current Density

E= Effective electric field

q = Charge of the electron

$\emptyset$ = Work function

q$\emptyset$= Height of the potential barrier

1D nanostructures field emitters and FN equation:

FN equation derivation includes the assumption that the surface of the sample is flat and the effective electric field E is same everywhere. But in carbon nanotubes the tip is sharp therefore the electric field distributions is different at the tip and have higher surface charge density. Due to this increased electric field near the tip, the **field enhancement factor$\boldsymbol{\beta}$,** is introduced. Therefore the effective or local field near the tip can be expressed as,

$E = \beta E_{avg}$

where,

E_{avg} = Average electric field

For a parallel plate electrode configuration E_{avg} is given by

$E_{avg} = \frac{V}{d_0}$

Where,

V= Voltage applied between the planar parallel plate electrode

d_0= Distance separating the two electrodes

β is always be greater than 1 for Carbon nanotubes since the surface charge density at the tip is higher than that of the tube and hence the effective field is greater than the average field.

This is why carbon nanotubes can be used as **Field Emitters**. Application of the same electric field will give a higher effective field which in turn increase the field emission current density. Smaller the diameter of the tip better will be the field emitting property. The macroscopic field emission is dependent on length of the carbon nanotubes and the density. Low density sample show non homogeneous emission pattern and low emission current.

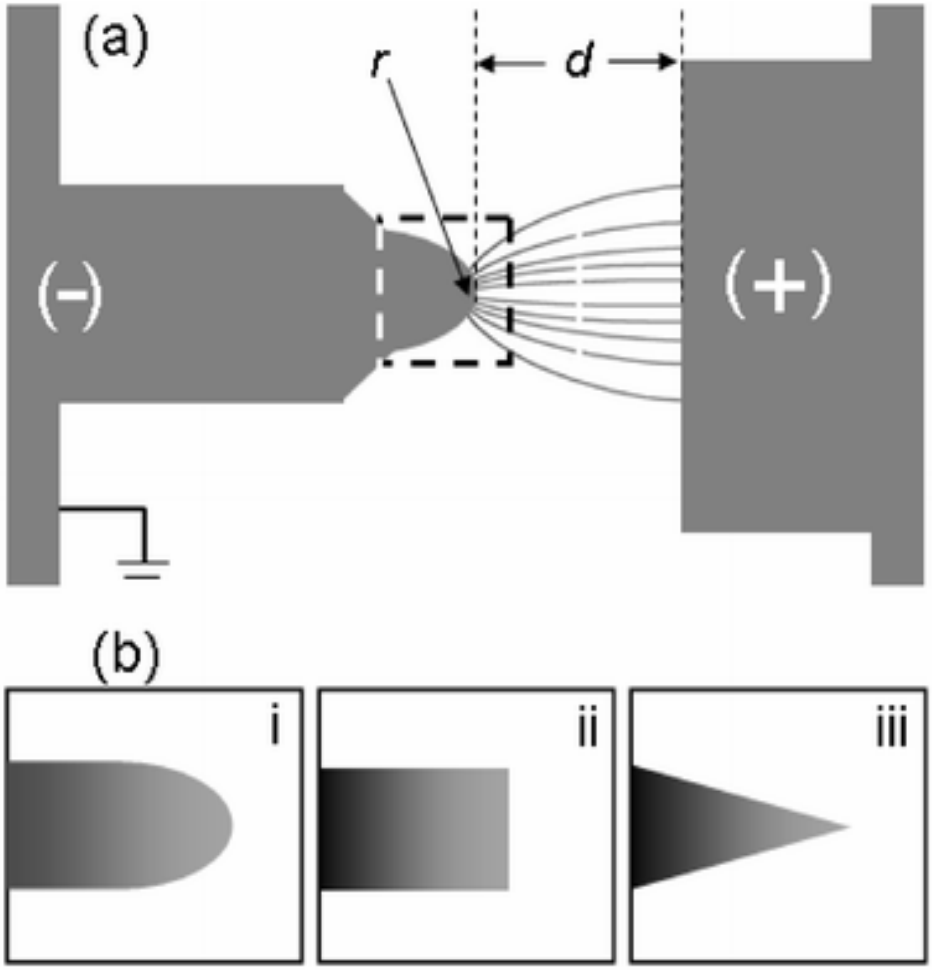

Fig1.4.5 (ii) (a) Field Emission Phenomena occurring at the tip of the emitter (b)Emission from (i) round tip (ii) Blunt tip (iii) Sharp tip or Conical tip

1.5 DIFFERENT METHODS OF SYNTHESIS OF CARBON NANOTUBES

There are basically three primary methods of synthesis of Carbon nanotubes which are listed below,

(i) Arc Discharge

(ii) Laser Ablation

(iii) Chemical Vapour Deposition

(i) Arc Discharge

Arc Discharge method was first used by **Iijima** in 1991 which gives rise to new type of carbon nanostructure that are needle type tubes. Electron microscopy revealed them to be coaxial tubes. In this method CNTs are produced through the vaporization of two carbon rods that are placed end to end separated by a distance about 1mm in an enclosure which is filled with inert gas (Helium or Argon) at low pressure (50-700mbar).The carbon rods used are acting as electrodes and a potential difference of 20V is applied which causes a DC of 50-100A. This direct current causes a high temperature discharge between the electrodes which results in vaporization of the surface of one of the electrode and deposition of the carbon vapour at the other electrode. Though the method is a simple one but it produces mixture of components which further needs to be filtration. Temperature of the deposits and the uniformity of the plasma arc decide the yield of the CNTs. Due to the high temperature about 28% of anode also gets evaporated.

(ii) Laser Ablation

Laser Ablation was first used by **Richard E. Smalley** and his group in 1995. Intense Laser is used to ablate the carbon target which is placed in the tube furnace heated to 1200°. The CNTs formed are carried towards the copper collector by the inert gas which is flown inside the tube. The CNTs formed are collected when the tube gets cooled down.

The above two method uses pure carbon which leads to the formation of MWNTs but in presence of catalyst (iron, sulphur, molybdenum) gives SWNTs.

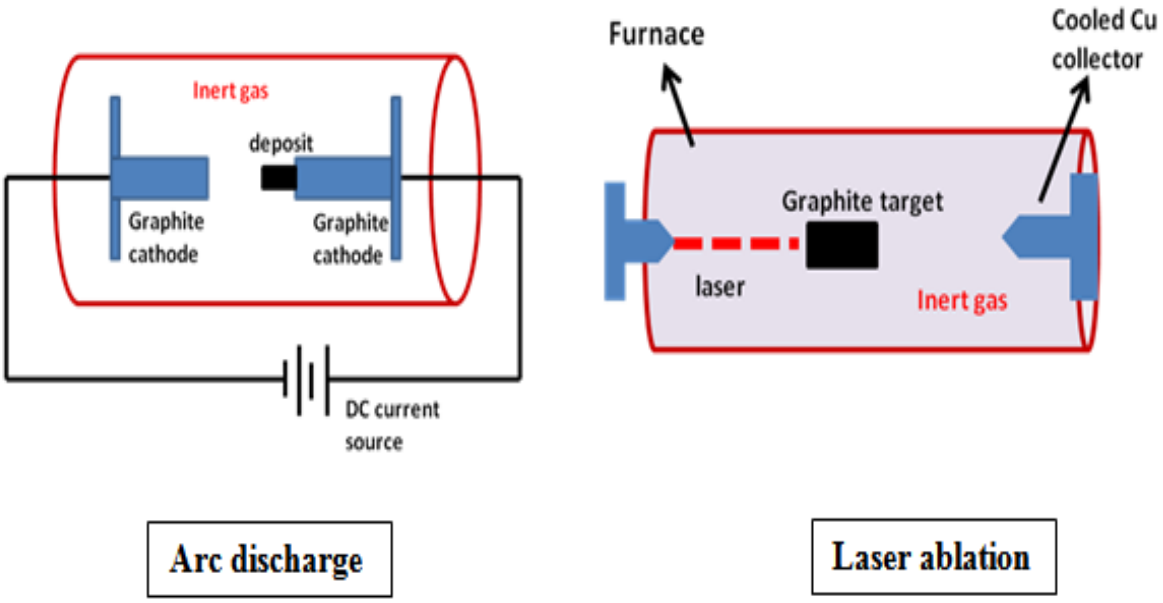

Fig1.5: (i)Arc discharge method and (ii)Laser ablation

(iii) Chemical Vapour Deposition

In 1993, carbon nanotubes were first synthesized by this method. A chamber is present which is heated up to a temperature of 700° . In this same chamber a substrate covered with a metal catalyst like iron and nickel is present. Two gases are introduced, one is the carrier gas like nitrogen and the other is hydrocarbon gas like methane. In this process production of carbon nanotubes reaches up to 90%. A lot of research is going on in this area. In 2006, a low temperature CVD having tungsten filament is reported which can synthesize single walled CNTs at a temperature as low as 350°[44]. In 2007, a highly efficient CVD method was demonstrated which is also environment friendly [43]

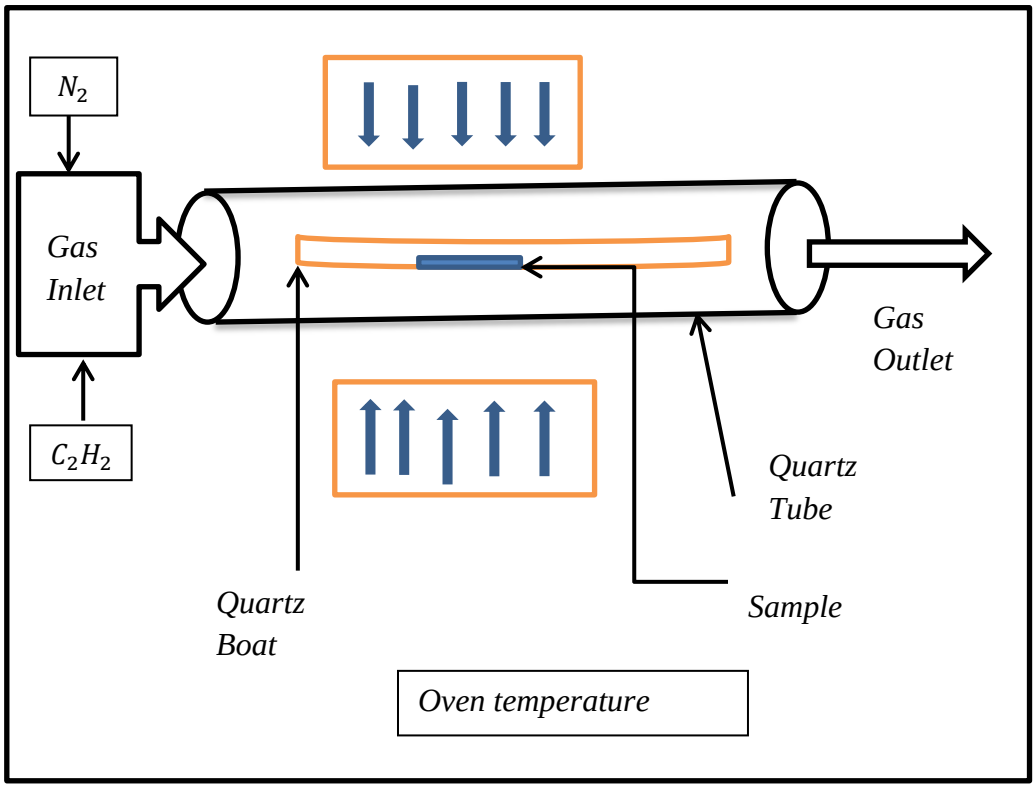

Fig 1.5 (iii) A schematic diagram of chemical vapour deposition

1.6 APPLICATION OF CABON NANOTUBES

The amazing and special properties of CNTs have encouraged researchers to use them in various fields for the betterment of mankind. Some of the applications are listed below,

(i) Energy application:

CNTs are used as 3D structured electrodes.

(a) In Li-ion batteries→Si coated CNT as anode electrode.

(b) Catalyst made from nitrogen doped CNTs.

(c) CNT can be used as a catalyst in fuel cells.

(ii) Carbon nanotubes in medical application:

Dental implants are improved by adding nanotubes to the surface of the implant materials. Scientists have developed sensors that can track the level of nitric acid present in the bloodstream by simply injecting the sensor within the skin. Artificial muscles have also been

demonstrated by the researchers that are made up of CNTs. CNTs shows the capability to bound itself with an antibody that are useful in destroying breast cancer tumours in lab tests.

(iii) Carbon nanotubes in Electronics:

Integrated circuits are built from the nanotube transistors. CNTs are used as Nano emissive display panels, printable electronics using nanotube as ink, transparent and flexible electronic devices using arrays of nanotubes.

(iv) Carbon nanotubes and environment:

Addition of Boron atoms during the growth of the CNT gives rise to sponge like CNT which can be used to clean the oil spills. Carbon nanotubes can be used as a sensor to sense chemical vapour. They can be used as pores in the membrane and helps in reverse osmosis desalination plants. Carbon nanotubes having gold tips can be used to trap oil drops.

CHAPTER 2: LITERATURE REVIEW

2.1 INTRODUCTION

Contribution and works of various researchers and scientists in the field of field emission, field emission properties, morphological features affecting the field emission, field enhancement factor for single CNT and an array of CNTs, effect of screening on field enhancement factor etc. are discussed in this chapter.

In Section 1, the basic of field emission and how CNTs can be used as field emitters is dealt. In Section 2, we would see how morphological features affect the field emission (effect on field enhancement factor). Finally in Section 3, we would see the effect of other CNTs on a single CNT present in an array of CNTs.

2.2 STUDY OF FIELD EMISSION AND USE OF CNTs AS FIELD EMITTERS BY VARIOUS AUTHORS

Basics and theory of field emission is already discussed in chapter 1. Here we would see an overview of research going on in the field of field emission and use of CNT field emitters and their potential applications.

Bonard *et al.* [1] demonstrated the systematic studies of field emission characteristics of different types of carbon nanotubes (single walled, multi walled nanotubes grown by closed and opened arc method and also by the help catalyst) as single emitters and film form and they confirmed excellent field emission properties. They have also discussed the field enhancement factor that has risen from the small radius of CNT tip is somehow responsible for the good emission.

Saito *et al*. [2] have described the field emission pattern, current voltage characteristics and F-N plots for both MWNTs and SWNTs.They have also manufactured cathode ray tube type lighting elements and vacuum fluorescence display panels to show the application of nanotube field emitters, have used MWNTs field emitters in place of thermionic cathodes which showed electron emission to be stable, adequate luminance and emitters life to be long.

Lee *et al*. [3] revealed the threshold electric field for excellent field emission characteristics to be $2V/\mu m$,when field emission displays based on carbon nanotubes (SWNTs) were integrated to describe the moving colour images. They have also investigated triode type

display structure which showed the electron emission could be controlled by gate voltage modulation.

Kim *et al.* [4] have fabricated Carbon nanotube (CNT) field emission displays (FED) which are scalable at 415℃ , brightness as high as 1800 cd/m^2 with a turn on field of 1V/mm and 1.5mA field emission current at 3V/mm and also current fluctuation is about 7% only. They have concluded that the high field enhancement factor with a low turn on field is due to the well aligned carbon nanotubes.

Cheng *et al.* [5] have also discussed the emission characteristics of CNT cathodes and the properties which are responsible for it. They have briefed the issues regarding the applications of CNT based cold cathodes in vacuum microelectronics devices.

Baughman *et al.* [6] have discoursed the various potential applications of carbon nanotubes and the barriers (cost, poly dispersity and the limitations in processing and assembly methods) which are there.

Chen *et al*. [7] have reported that the field emission of the CNTs varies depending upon the orientation to their substrate (45°, parallel and perpendicular). It was reported that field emission occurs from the wall of the tube also and the reason behind the emission of electron from the surface of the tube wall is discussed.

2.3 STUDY OF MORPHOLOGICAL AND OTHER FACTORS AFFECTING THE FIELD EMISSION BY VARIOUS AUTHORS

Zhou *et al*. [8] have studied open ended SWNTs and their field emission mechanism and drew the conclusion that an open ended SWNT has better field emission properties compared to that of closed SWNT. The geometrical and the electronic structure effects the work function and the amplification factor. It was also suggested that by varying electronically and geometrically, the localized electronic states of the emitting regions field emission properties of the nanotubes can be improved.

Srivastava *et al.* [9] have discussed how the morphological features of the substrate can affect the field emission properties of carbon nanotube films. CNT films of different morphological structures were studied and it was found that the patterned CNT films and that are with randomly oriented morphology have better emission characteristics and have threshold field as 2.0V/μm.

Smith *et al.* [10] have showed by computational simulation how the aspect ratio and the location of anode effects the field emission properties of single tip based emitter. According to them if the anode and cathode are separated three times the height of the emitter from the tip of the emitter then only the field enhancement factor is dependent on the radius of curvature of the tip and the emitter height (if D>3h then only β is dependent on r and h).The field enhancement factor is expressed as $\beta_0 = \left(1 + \sqrt{\frac{h}{\alpha r}}\right)^m$ where α=2 and m=1.

Wang *et al*. [11] have showed the emission tip structures highly effect the electron emission properties. They have particularly studied the field emission characteristics when a capped CNT is converted to an opened CNT and vice versa by removal of carbon atoms from the tip in controlled manner.

Xu *et al*. [12] have utilized *in situ* transmission electron microscopy to measure the field emission properties of the MWNTs which showed that structure and the surface condition are the factors on which the work function at the nanotube tip depends.

Zhu *et al.* [14] have reported CNTs exhibit very good emission properties. Current densities of 10mA/cm^2 can be emitted by the application of the electric field as low as 4V/μm.The durability and good emission characteristic offer promising application in the field of vacuum microelectronics.

Zhang *et al*. [15] have studied and found that the interaction between the CNTs and the substrate plays an important role in the field emission process. They have taken a double barrier model to see the field emission of CNT films and reported that emission performance is highly affected by the width of the interface barrier.

Vink *et al.*[16]have reported a method to change the morphology of the CNTs by mechanical surface modification and have observed a homogeneous emission from the emitter surface with a emitter sites densities of 104 emitters/ cm^2 and extracted current densities 500 mA /cm^2.

Chan *et al*. [17] have shown that when MWNTs are doped with some extrinsic atoms the field emission properties are enhanced. When CNTs are doped with Nitrogen it increases the electron densities and when doped with Boron it increases the electron hole concentration thus resulting in the formation of electron traps and their F-N plots gives to different slopes.

Enhanced field emission properties are shown by **Green** *et al*. [18] when CNTs were coated with the ZnO. No significant change in the internal structures and diameter of the CNTs. ZnO provides additional sites for the emission of electrons and hence there occurs a enhancement in the field emission.

2.3 STUDY OF MODELING AND CALCULATION OF FIELD ENHANCEMENT FACTOR WITH AND WITHOUT SCREENING EFFECT BY VARIOUS AUTHORS.

Yoon *et al.* [13] have studied the field emission by varying the tube height of highly ordered nanotubes from the closed and open tips. Screening effect due to the neighbouring nanotubes effects the field emission from both kinds of tip and the field emission from the closed tip nanotubes are much more superior that of open ones.

Suh *et al*. [19] have studied and found that the field screening effect is encouraged by the proximity of the nanotubes that are present in the neighbourhood. By changing the height of the tube the field emission can be affected. It was also found that when the tube height is similar to the distance between the nanotubes field emission is optimum.

Wong *et al.* [20] have given an approach in which by adjusting the geometry, size and spacing in the array the efficiency of the field emitters can be enhanced. MPECVD is used to fabricate micro patterned CNT arrays that are vertically aligned with various geometries, sizes and spacing. Circular array showed the lowest turn-on field and achieves highest current density .The results verifies that by optimizing the spacing in the arrays of the CNT emitters could result lower turn on field and higher current density.

Jo *et al*. [21] investigated the effect of variation of length and spacing of the carbon nanotube independently on the field emission characteristics. By increasing the length and spacing of CNTs macroscopic electric field can be reduced. For very high density CNT films increase in length increases macroscopic electric field but for short CNT films, increase in spacing does not reduce the macroscopic electric field.

Wang *et al.* [22] have suggested a model in which a floating sphere between the anode and cathode plates was taken to estimate the field enhancement factor. The field enhancement factor was found out to be $\beta = \frac{h}{r} + 3.5 + A\left(\frac{h}{d}\right)^3$ where A is the constant; d is the distance between the anode and cathode, h is the height of the carbon nanotube. The main factors

which causes strong field at the apex are the higher aspect ratio and lower anode cathode distance.

Wang *et al*. [23] have also studied the model for carbon nanotube arrays and calculated the field emission factor. The expression of field enhancement factor for single CNT

$\beta_0 = \frac{h}{\rho} + 3.5$, where h and ρ are the height and radius of the CNT respectively was modified to $\beta_0 = \frac{h}{\rho} + 3.5 - W$ where W is the coulomb field interaction which also depends upon the inter-tube distance. Field emission is critically affected by the inter-tube distance of the CNTs array.

Wang *et al.* [24] optimized the field emission by numerical simulation. The simulated results showed that the emission current density is less whereas enhancement factor is highest for single CNT. As the inter-tube distance is decreased the field enhancement factor is decreased for the CNTs in array due to the introduction of screening effect. Simulation of capped and opened CNTs array showed distance between anode and cathode can affect the distribution of potential to some extent. Opened CNTs array showed larger field enhancement factor, thus can emit more current than the capped CNTs.

CHAPTER 3: RESEARCH WORK

Topic: Model calculation of field enhancement factor of CNTs having conical tip taking into account the shielding effect.

3.1 INTRODUCTION

CNTs are one of the strong competitors in the field of field emission and its application because of their unique and extraordinary properties of high aspect ratio, high mechanical strength, chemical inertness, right chemical stability which is mainly due to the electronic structure. Generally the tip of the CNT is considered as hemisphere and the field emission takes place from the tip and the field enhancement factor associated with it is estimated by considering simple models like 'hemisphere on a post' and 'floating sphere at emitter-plane potential'[25]. The field enhancement factor is given by the expression $\beta_0 = \frac{h}{\rho} + 3.5$ for single CNT [23] but when this single CNT is placed in a group/ cluster of CNTs the field enhancement factor is reduced due to the screening offered by the CNTs present nearby it [26].As the nanotubes tips are sharpened, there is dramatic increase in the field enhancement factor. So here we have proposed an electrostatic model for field emission from the conical tip of the CNT in which the effect of image charge is also considered.

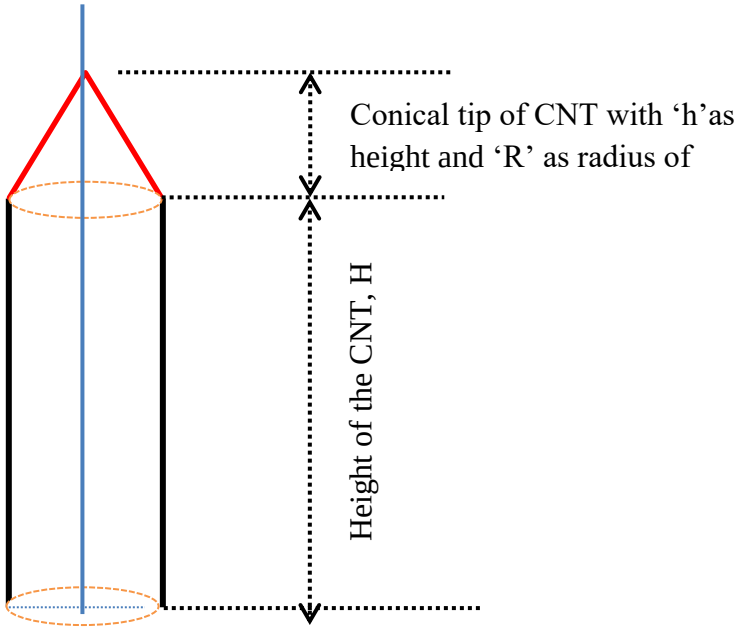

Fig3.1(i): Schematic diagram of CNT under consideration

3.2 RESEARCH METHODOLOGY

Model: Following **Wang** *et al.* [23] and **Ahmad** *et al.* [25] we will consider the effect of image charge effect. For the calculation of potential at any point in the space is shown in the model given below;

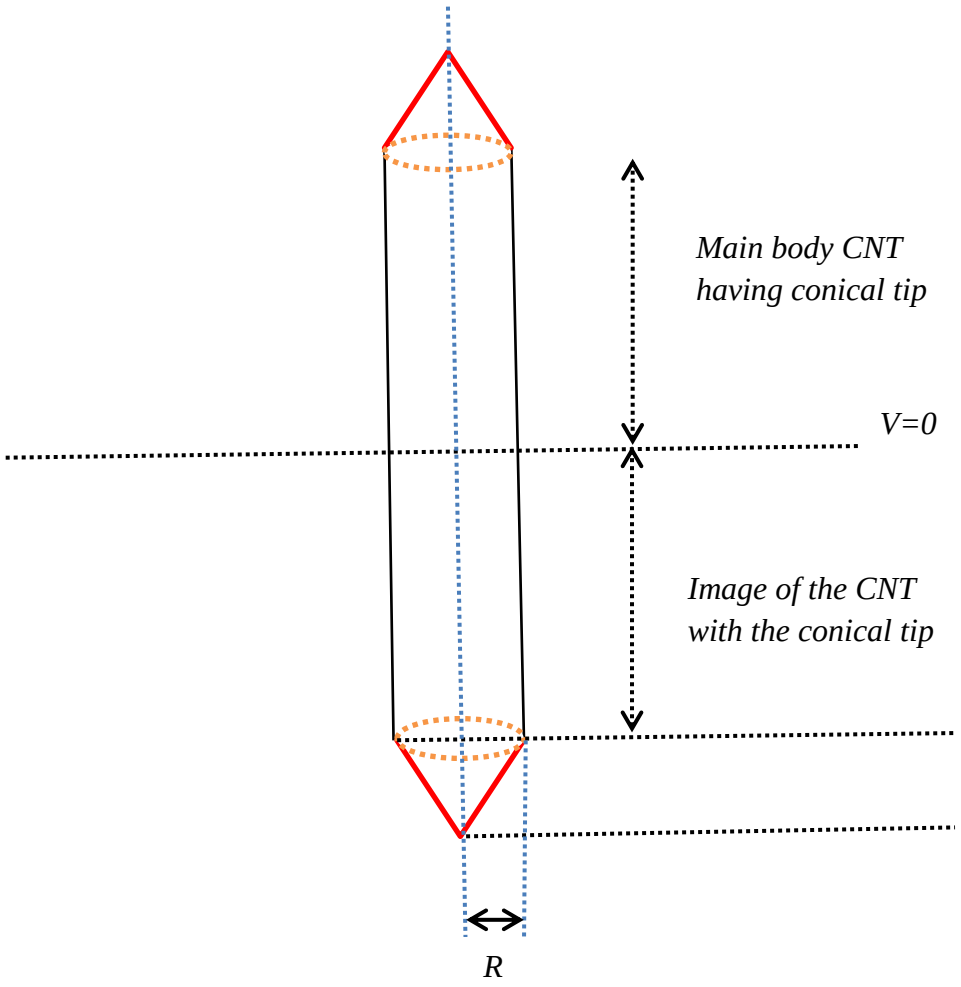

Fig 3.2(ii): Schematic diagram of the CNT under consideration with its image part

The emission of electron takes place from the tip of the nanotube therefore we will calculate the potential at any point in space P(x, 0, y) due to the upper conical tip and then we will be calculating for the image part.

Potential of the cone at any point:

The base of the cone is on x-y plane having radius R its centre at point 0 and height of the cone is H is along z axis, taking a point P is located anywhere in space. Due to axial

symmetry we do not lose generality by calculating the potential at r = (x,0,z). A small elemental disc at some height, (H-h) from the base of the cone is taken. The differential height and the slant height of the elemental disc are taken as 'dh' and 'dl' respectively. The cone is uniformly charged and has a surface charge density as ' σ'. The opening angle of the cone is 'α'.

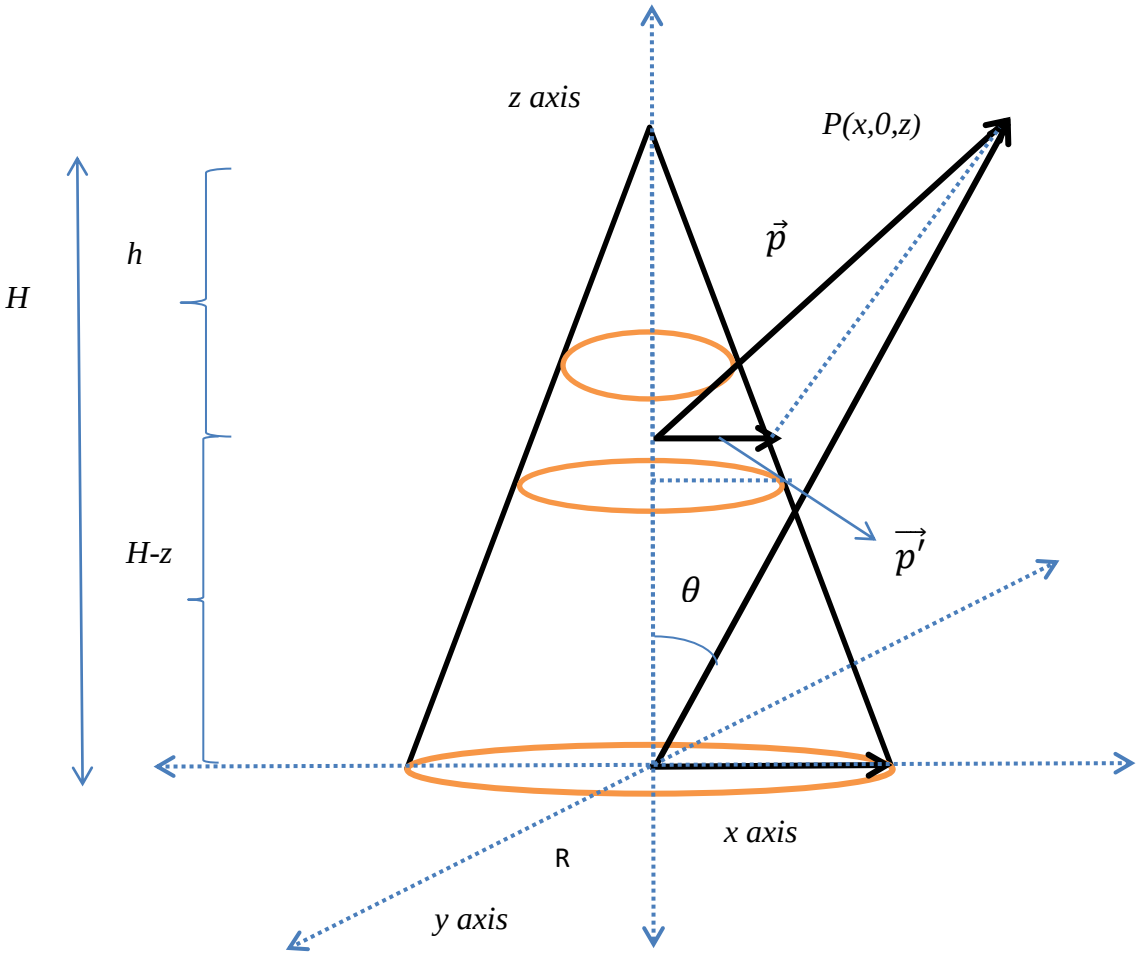

Fig3.2(iii): Schematic diagram of the conical tip under consideration-1

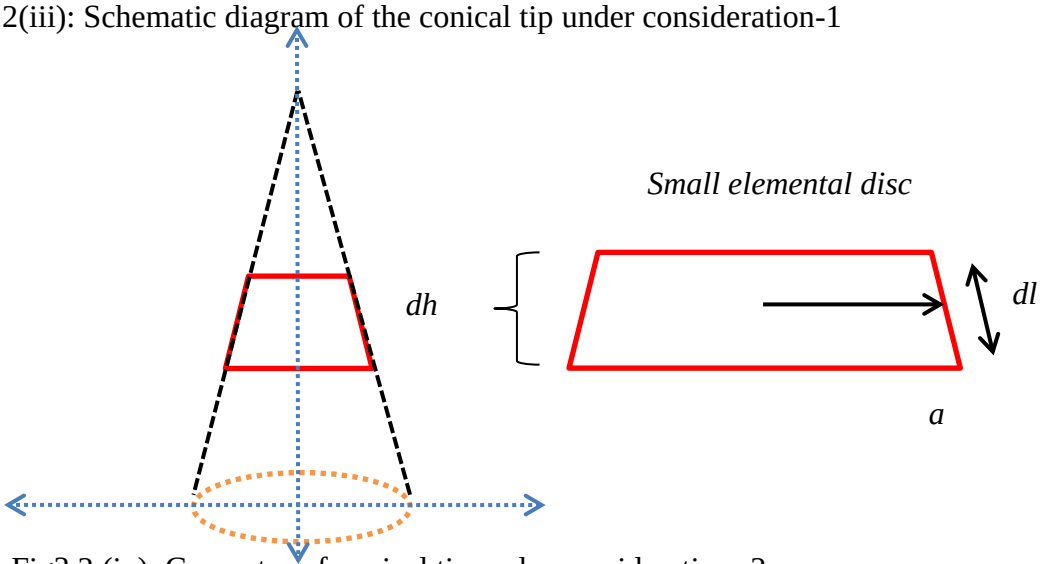

Fig3.2 (iv): Geometry of conical tip under consideration -2

Let the distance from the base of the cone to the arbitrary point P be r. This "r" can be written as,

$\vec{r} = x\hat{i} + z\hat{k}$

This $\vec{r}$ is making an angle θ with the z axis. Hence

$x = |\vec{r}| \sin\theta$

$z = |\vec{r}| \cos\theta$

Now let us take a vector from the centre of the small disc to that arbitrary point P as $\vec{p} = x\hat{i} + (z - (H - h))\hat{k}$

And another vector from the centre of the small disc to the surface of the cone as

$\overrightarrow{p'} = a\hat{i} + (H-h)\hat{k}$

$\left|\vec{p} - \overrightarrow{p'}\right| = \sqrt{(x - a)^2 + (z - (H - h) - (H - h))^2}$

On expanding and putting value of x and z in the above equation we obtain,

$\left|\vec{p} - \overrightarrow{p'}\right| = \sqrt{r^2 + (p')^2 - 2(r\sin\theta)a - 4(r\cos\theta)H + 4(r\cos\theta)h + 3(H - h)^2}$

Taking r^2 common,

$$\left|\vec{p} - \overrightarrow{p'}\right| = r\sqrt{1 + \left(\frac{p'}{r}\right)^2 - 2\left(\frac{a}{r}\right)\sin\theta - 4\left(\frac{H}{r}\right)\cos\theta + 4\left(\frac{h}{r}\right)\cos\theta + 3\left(\frac{H - h}{r}\right)^2}$$

Now,

$\frac{a}{h} = \tan\alpha$, where α is the opening angle of the cone

$a = h\tan\alpha$

$$dV = \frac{1}{4\pi\varepsilon_0}\frac{dq}{\left|\vec{p} - \overrightarrow{p'}\right|} \qquad (1)$$

$dq = \sigma dA$, where σ and dA are surface charge density and differential area respectively.

$dA = 2\pi a dl$, where dl is the differential slant height of the elemental disc.

$$\frac{dh}{dl} = \cos\alpha$$

$$dl = dh\ \sec\alpha$$

Therefore, $da = 2\pi a(dh\ \sec\alpha)$

After putting value of 'a' we obtain

$$dq = \sigma(2\pi)(h\tan\alpha)(\sec\alpha\ dh)$$

$$dV = \frac{1}{4\pi\varepsilon_0}\frac{\sigma(2\pi)(h\tan\alpha)(\sec\alpha\ dh)}{r\sqrt{1+\left(\frac{p'}{r}\right)^2 - 2\left(\frac{a}{r}\right)\sin\theta - 4\left(\frac{H}{r}\right)\cos\theta + 4\left(\frac{h}{r}\right)\cos\theta + 3\left(\frac{H-h}{r}\right)^2}}$$

Neglecting $\left(\frac{p'}{r}\right)^2$ and $3\left(\frac{H-h}{r}\right)^2$ and expanding binomially we obtain,

$$dV = \frac{1}{4\pi\varepsilon_0}\frac{2\pi\sigma\sec\alpha\tan\alpha}{r}\ h\ dh\left(1+\frac{h}{r}\tan\alpha\sin\theta + 2\frac{H}{r}\cos\theta - 2\frac{h}{r}\cos\theta\right)$$

Now integrating on both side,

$$V = \frac{1}{4\pi\varepsilon_0}\frac{2\pi\sigma\sec\alpha\tan\alpha}{r}\left(\frac{H^2}{2} + \frac{H^3\tan\alpha\sin\theta}{3r} + \frac{H^3\cos\theta}{r} - 2\frac{H^3\cos\theta}{3r}\right)$$

Putting the value of σ, $\tan\alpha$ and $\sec\alpha$ i.e

$$\sigma = \frac{Q}{\pi Rl}$$

$$\tan\alpha = \frac{R}{H}\ \text{ and }\ \sec\alpha = \frac{l}{H}$$

$$V = \frac{1}{4\pi\varepsilon_0}Q\left(\frac{1}{r} + \frac{2}{3}\frac{R\sin\theta}{r^2} + \frac{2}{3}\frac{H\cos\theta}{r^2}\right) \qquad (2)$$

Calculation of field enhancement factor:

Wang *et al*. [23] and **Ahmad** *et al*. [25] have followed the mirror method to calculate the electric field at the apex of the carbon nanotube. A charge $-Q$ and $-P$ in the vertical direction are assumed at the conical tip and the image charge $+Q$ and image potential $+P$ were introduced at the symmetric point in order to keep the cathode at ground potential. Let the length of the CNT be"h'"and radius "R" and the CNT has a conical tip of height "H" and radius of the base "R".A voltage of V_a is applied at the anode plate and the cathode plate is at 0 potential. The cathode and the anode are separated by a distance "d".

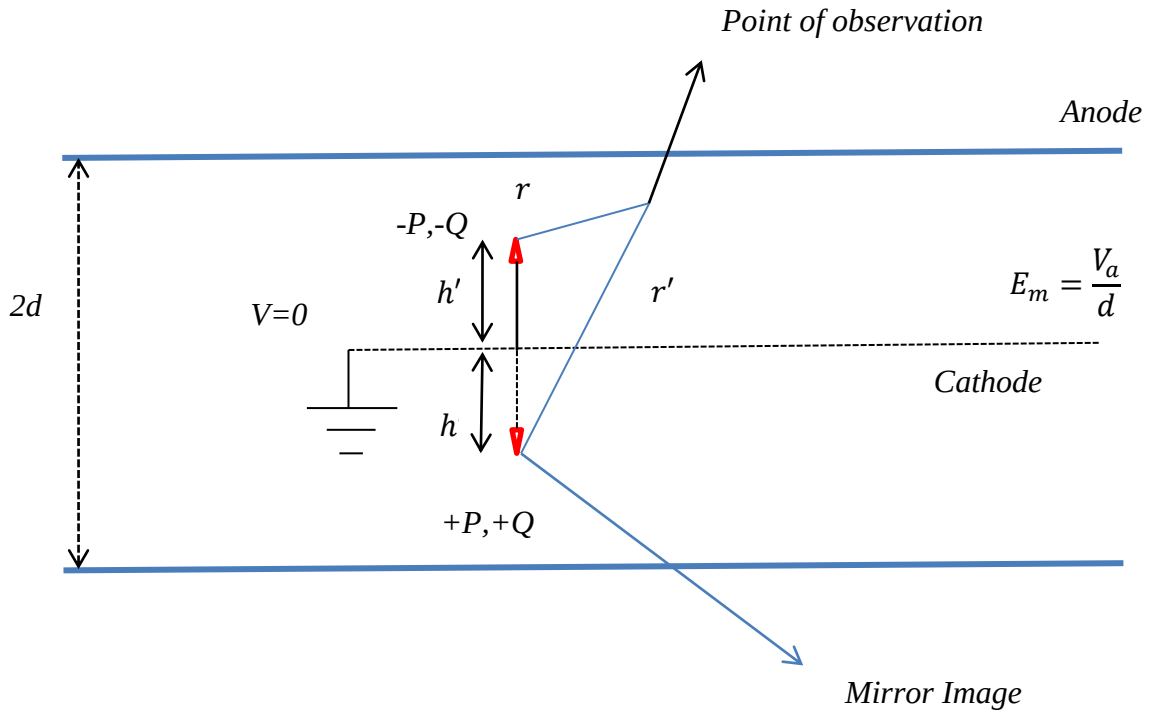

Fig3.2 (v) Model for the field emission of a CNT with induced charge and its mirror image

Let (r, θ) denote the spherical coordinates of any point in space near the top of the cone. Then the potential at this point should be

$$\varphi(r,\theta)=\frac{1}{4\pi\varepsilon_0}\left\{-Q\left(\frac{1}{r}+\frac{2}{3}\frac{R\sin\theta}{r^2}+\frac{2}{3}\frac{H\cos\theta}{r^2}\right)-\frac{P\cos\theta}{r^2}\right.$$
$$\left.+Q\left(\frac{1}{r'}+\frac{2}{3}\frac{R\sin\theta'}{r'^2}+\frac{2}{3}\frac{H\cos\theta'}{r'^2}\right)+\frac{P\cos\theta'}{r'^2}\right\}+E_m(h'+r\cos\theta) \quad (3)$$

Neglecting terms having r'^2 term in the denominator and substituting $\frac{1}{r'}\approx\frac{1}{2h'}$

$$\varphi(r,\theta)=\frac{1}{4\pi\varepsilon_0}\left\{-Q\left(\frac{1}{r}+\frac{2}{3}\frac{R\sin\theta}{r^2}+\frac{2}{3}\frac{H\cos\theta}{r^2}\right)-\frac{P\cos\theta}{r^2}+Q\left(\frac{1}{r'}\right)\right\}+E_m(h'\ +r\cos\theta)$$

Demanding $\varphi(r,\theta)=0$ at $\theta=0$ and $r=H$

$$0=\frac{1}{4\pi\varepsilon_0}\left\{-Q\left(\frac{1}{H}+\frac{2}{3H}\right)-\frac{P}{H^2}+Q\left(\frac{1}{2h'}\right)\right\}+E_m(h'+H)$$

$$P=H^2\left\{E_m(h'+H)(4\pi\varepsilon_0)-Q\frac{(10h'-3H)}{6Hh'}\right\} \quad (4)$$

Further $\varphi(r,\theta)=0$ at $\theta=90$ and $r=R$

$$0=\frac{1}{4\pi\varepsilon_0}\left\{-Q\left(\frac{1}{R}+\frac{2}{3R}\right)+Q\left(\frac{1}{2h'}\right)\right\}+E_m(h')$$

$$Q=\frac{3}{5}(E_m h')(4\pi\varepsilon_0)R\left(1+\frac{3R}{10h'}\right) \quad (5)$$

Putting the value of Q in equation (3) we obtain the value of P

$$P=H^2\left\{E_m(h'+H)(4\pi\varepsilon_0)-\frac{3}{5}(E_m h')(4\pi\varepsilon_0)R\left(1+\frac{3R}{10h'}\right)\left(\frac{10h'-3H}{6Hh'}\right)\right\} \quad (6)$$

The field strength at the top of the cone,

$$E_0=-\left[\frac{d\varphi(r,\theta=0)}{dr}\right]_{r=H}$$

$$E_0=-\left[\frac{1}{4\pi\varepsilon_0}\left(\frac{7Q}{3H^2}+\frac{2P}{H^3}\right)+E_m\right] \quad (7)$$

Putting value of Q and P in equation (7) we obtain the expression for field enhancement factor without screening as,

$$\beta_0 = -\left\{2\left(\frac{h'}{H}\right) - \frac{3}{5}\left(\frac{h'}{H}\right)\left(\frac{R}{H}\right) - \frac{9}{50}\left(\frac{R}{H}\right)^2 + \frac{3}{5}\left(\frac{R}{H}\right) + \frac{9}{50}\left(\frac{R}{H}\right)\left(\frac{R}{h'}\right) + 3\right\} \quad (8)$$

Calculation of the field enhancement factor taking into account the shielding effect:

Now we will consider cluster of CNTs so that screening effect can be taken into account. Each nanotube tip will have charge –Q and dipole moment –P and their mirror image will have charge +Q and dipole moment +P. Distance between the nth CNTs and the CNT under consideration as r_n and it can be written as,

$r_n = \sqrt{x_n^2 + y_n^2}$, where (x_n, y_n) are the coordinates of the base of the CNTs w.r.t the base of the CNT under consideration and $r_n >> r$.

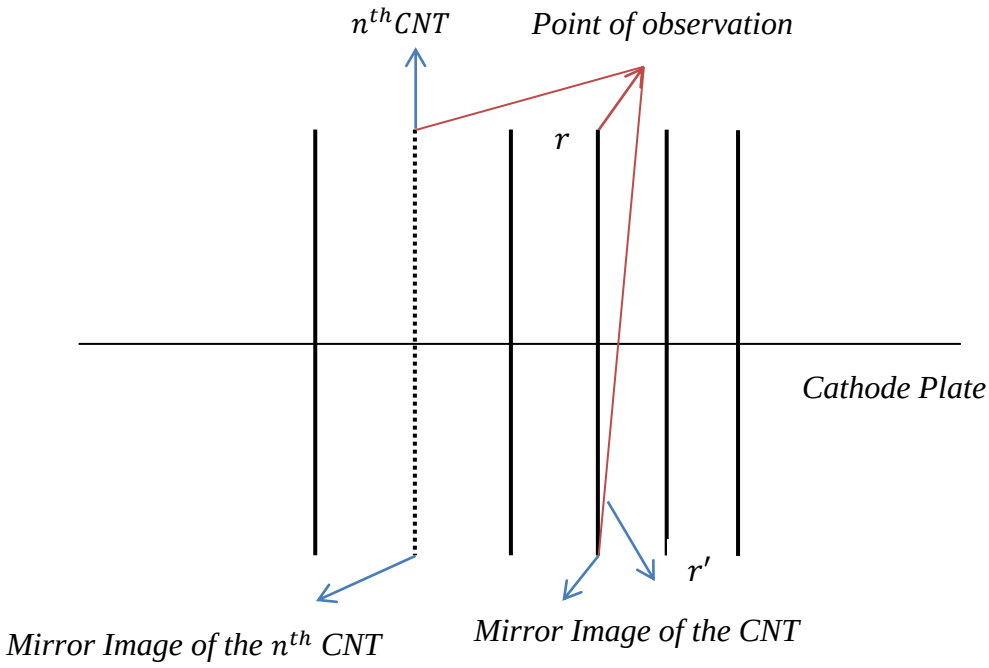

Fig3.2 (v) Distribution of CNTs

The electrostatic potential can be written as,

$$\varphi(r,\theta) = \frac{1}{4\pi\varepsilon_0}\left\{-Q\left(\frac{1}{r}+\frac{2}{3}\frac{R\sin\theta}{r^2}+\frac{2}{3}\frac{H\cos\theta}{r^2}\right)-\frac{P\cos\theta}{r^2}+Q\left(\frac{1}{2h'}\right)\right.$$
$$\left.+\sum_{n=1}^{m}-Q\left(\frac{1}{r_n}+\frac{2}{3}\frac{R\sin\theta_n}{{r_n}^2}+\frac{1}{3}\frac{H\cos\theta_n}{{r_n}^2}\right)+\sum_{n=1}^{m}Q\left(\frac{1}{\sqrt{{r_n}^2+(2h')^2}}\right)\right\}$$
$$+E_m(h'+r\cos\theta) \qquad (9)$$

Since we are interested in the electric field in the proximity of CNT $r_n \gg r$ therefore above equation can be written as

$$\varphi(r,\theta) = \frac{1}{4\pi\varepsilon_0}\left\{-Q\left(\frac{1}{r}+\frac{2}{3}\frac{R\sin\theta}{r^2}+\frac{2}{3}\frac{H\cos\theta}{r^2}\right)-\frac{P\cos\theta}{r^2}+Q\left(\frac{1}{2h'}\right)+\sum_{n=1}^{m}-Q\left(\frac{1}{r_n}\right)\right.$$
$$\left.+\sum_{n=1}^{m}Q\left(\frac{1}{\sqrt{{r_n}^2+(2h')^2}}\right)\right\}+E_m(h'+r\cos\theta)$$

Demanding $\varphi(r,\theta)=0$ at $\theta=0$ and $r=H$

$$0 = \frac{1}{4\pi\varepsilon_0}\left\{-Q\left(\frac{1}{H}+\frac{2}{3H}\right)-\frac{P}{H^2}+Q\left(\frac{1}{2h'}\right)+\sum_{n=1}^{m}-Q\left(\frac{1}{r_n}\right)+\sum_{n=1}^{m}Q\left(\frac{1}{\sqrt{{r_n}^2+(2h')^2}}\right)\right\}$$
$$+E_m(h'+H)$$

$$E_m(h'+H) = \frac{1}{4\pi\varepsilon_0}\left\{Q\left(\frac{1}{H}+\frac{2}{3H}\right)+\frac{P}{H^2}-Q\left(\frac{1}{2h'}\right)-\sum_{n=1}^{m}-Q\left(\frac{1}{r_n}\right)\right.$$
$$\left.-\sum_{n=1}^{m}Q\left(\frac{1}{\sqrt{{r_n}^2+(2h')^2}}\right)\right\} \qquad (10)$$

Further $\varphi(r,\theta)=0$ at $\theta=90$ and $r=R$

$$0 = \frac{1}{4\pi\varepsilon_0}\left\{-Q\left(\frac{1}{R}+\frac{2}{3R}\right)+Q\left(\frac{1}{2h'}\right)+\sum_{n=1}^{m}-Q\left(\frac{1}{r_n}\right)+\sum_{n=1}^{m}Q\left(\frac{1}{\sqrt{{r_n}^2+(2h')^2}}\right)\right\}+E_m(H)$$

$$E_m(H) = \frac{1}{4\pi\varepsilon_0}\left\{Q\left(\frac{1}{R}+\frac{2}{3R}\right)-Q\left(\frac{1}{2h'}\right)-\sum_{n=1}^{m}-Q\left(\frac{1}{r_n}+\frac{2}{3}\frac{R}{{r_n}^2}\right)-\sum_{n=1}^{m}Q\left(\frac{1}{\sqrt{{r_n}^2+(2h')^2}}\right)\right\}$$

On solving we obtain,

$$Q = \left(\frac{3R}{5}\right)(E_m h')(4\pi\varepsilon_0)\left(1 + \frac{3}{10}\frac{R}{h'} - \frac{3R}{5}\sum_{n=1}^{m}\left(\frac{1}{r_n}\right) + \frac{3R}{5}\sum_{n=1}^{m}\left(\frac{1}{\sqrt{{r_n}^2 + (2h')^2}}\right)\right)$$

Putting value of Q in equation (10) we will get the value of P as

$$P = H^2\Bigg\{E_m(h' + H)(4\pi\varepsilon_0) - \left[\left(\frac{3R}{5}\right)(E_m h')(4\pi\varepsilon_0)\left(1 + \frac{3}{10}\frac{R}{h'} - \frac{3R}{5}\sum_{n=1}^{m}\left(\frac{1}{r_n}\right) + \frac{3R}{5}\sum_{n=1}^{m}\left(\frac{1}{\sqrt{{r_n}^2 + (2h')^2}}\right)\right)\right]\left[\frac{5}{3H} - \frac{1}{2h'} + \sum_{n=1}^{m}\left(\frac{1}{r_n}\right) - \sum_{n=1}^{m}\left(\frac{1}{\sqrt{{r_n}^2 + (2h')^2}}\right)\right]\Bigg\}$$

$$E_0 = -\left[\frac{d\varphi(r, \theta = 0)}{dr}\right]_{r=H}$$

$$E_0 = -\left[\frac{1}{4\pi\varepsilon_0}\left(\frac{7Q}{3H^2} + \frac{2P}{H^3}\right) + E_m\right] \tag{11}$$

Putting value of P and Q in equation (11)

$$
\begin{aligned}
E_0 = -E_m \Bigg\{ & 2\left(\frac{h'}{H}\right) - \frac{3}{5}\left(\frac{h'}{H}\right)\left(\frac{R}{H}\right) - \frac{9}{50}\left(\frac{R}{H}\right)^2 + \frac{3}{5}\left(\frac{R}{H}\right) + \frac{9}{50}\left(\frac{R}{H}\right)\left(\frac{R}{h'}\right) + 3 \\
& - \Bigg[\frac{21}{25}\left(\frac{h'}{H}\right)\left(\frac{R}{H}\right) R \sum_{n=1}^{m}\left(\frac{1}{r_n}\right) \\
& - \frac{21}{25}\left(\frac{h'}{H}\right)\left(\frac{R}{H}\right) R \sum_{n=1}^{m}\frac{1}{\sqrt{{r_n}^2 + (2h')^2}} \\
& + \frac{6}{5}\left(\frac{h'}{H}\right) R \sum_{n=1}^{m}\left(\frac{1}{r_n}\right) \\
& - \frac{6}{5}\left(\frac{h'}{H}\right) R \sum_{n=1}^{m}\frac{1}{\sqrt{{r_n}^2 + (2h')^2}} \\
& + \frac{9}{25}\frac{R}{H} R \sum_{n=1}^{m}\left(\frac{1}{r_n}\right) \\
& - \frac{9}{25}\frac{R}{H} R \sum_{n=1}^{m}\frac{1}{\sqrt{{r_n}^2 + (2h')^2}} \\
& - \frac{6}{5}\left(\frac{h'}{H}\right)\left(\frac{R}{H}\right) R \sum_{n=1}^{m}\left(\frac{1}{r_n}\right) + \frac{9}{25}\left(\frac{R}{H}\right) R \sum_{n=1}^{m}\left(\frac{1}{r_n}\right) \\
& - \frac{18}{25}\left(\frac{h'}{H}\right) R^2 \sum_{n=1}^{m}\left(\frac{1}{r_n}\right)\left(\frac{1}{r_n}\right) + \frac{18}{25}\left(\frac{h'}{H}\right) R^2 \sum_{n=1}^{m}\left(\frac{1}{r_n}\right)\left(\frac{1}{\sqrt{{r_n}^2 + (2h')^2}}\right) \\
& + \frac{6}{5}\left(\frac{h'}{H}\right)\left(\frac{R}{H}\right) R \sum_{n=1}^{m}\frac{1}{\sqrt{{r_n}^2 + (2h')^2}} - \frac{9}{25}\left(\frac{R}{H}\right) R \sum_{n=1}^{m}\left(\frac{1}{\sqrt{{r_n}^2 + (2h')^2}}\right) \\
& + \frac{18}{25}\left(\frac{h'}{H}\right) R^2 \sum_{n=1}^{m}\left(\frac{1}{\sqrt{{r_n}^2 + (2h')^2}}\right)\left(\frac{1}{r_n}\right) \\
& - \frac{18}{25}\left(\frac{h'}{H}\right) R^2 \sum_{n=1}^{m}\left(\frac{1}{{r_n}^2 + (2h')^2}\right) \Bigg] \Bigg\}
\end{aligned}
\tag{12}
$$

On solving the above equation and writing the expression in terms of β_0 we obtain,

$$\beta = -\left\{\beta_0 - \left[\frac{21}{25}\left(\frac{h'}{H}\right)\left(\frac{R}{H}\right)R\sum_{n=1}^{m}\left(\frac{1}{r_n}\right)\right.\right.$$
$$-\frac{21}{25}\left(\frac{h'}{H}\right)\left(\frac{R}{H}\right)R\sum_{n=1}^{m}\frac{1}{\sqrt{{r_n}^2+(2h')^2}}$$
$$+\frac{6}{5}\left(\frac{h'}{H}\right)R\sum_{n=1}^{m}\left(\frac{1}{r_n}\right)$$
$$-\frac{6}{5}\left(\frac{h'}{H}\right)R\sum_{n=1}^{m}\frac{1}{\sqrt{{r_n}^2+(2h')^2}}$$
$$+\frac{9}{25}\frac{R}{H}R\sum_{n=1}^{m}\left(\frac{1}{r_n}\right)$$
$$-\frac{9}{25}\frac{R}{H}R\sum_{n=1}^{m}\frac{1}{\sqrt{{r_n}^2+(2h')^2}}$$
$$-\frac{6}{5}\left(\frac{h'}{H}\right)\left(\frac{R}{H}\right)R\sum_{n=1}^{m}\left(\frac{1}{r_n}\right)+\frac{9}{25}\left(\frac{R}{H}\right)R\sum_{n=1}^{m}\left(\frac{1}{r_n}\right)$$
$$-\frac{18}{25}\left(\frac{h'}{H}\right)R^2\sum_{n=1}^{m}\left(\frac{1}{r_n}\right)\left(\frac{1}{r_n}\right)+\frac{18}{25}\left(\frac{h'}{H}\right)R^2\sum_{n=1}^{m}\left(\frac{1}{r_n}\right)\left(\frac{1}{\sqrt{{r_n}^2+(2h')^2}}\right)$$
$$+\frac{6}{5}\left(\frac{h'}{H}\right)\left(\frac{R}{H}\right)R\sum_{n=1}^{m}\frac{1}{\sqrt{{r_n}^2+(2h')^2}}-\frac{9}{25}\left(\frac{R}{H}\right)R\sum_{n=1}^{m}\left(\frac{1}{\sqrt{{r_n}^2+(2h')^2}}\right)$$
$$+\frac{18}{25}\left(\frac{h'}{H}\right)R^2\sum_{n=1}^{m}\left(\frac{1}{\sqrt{{r_n}^2+(2h')^2}}\right)\left(\frac{1}{r_n}\right)$$
$$\left.\left.-\frac{18}{25}\left(\frac{h'}{H}\right)R^2\sum_{n=1}^{m}\left(\frac{1}{{r_n}^2+(2h')^2}\right)\right]\right\} \qquad (13)$$

This expression can be used to determine the field enhancement factor at any position in the distribution of CNTs on a metallic surface.

The expression which we have derived can be used to compute the field enhancement factor of a CNT present in square the array which is uniformly spaced. Putting $r_n = s\sqrt{a^2 + b^2}$ where "s" is the distance between the CNTs a and b are integers.

Neglecting some terms the final expression,

$$\beta = -\left\{\beta_0 - \left[\frac{21}{25}\left(\frac{h'}{H}\right)\left(\frac{R}{H}\right)\left(\frac{R}{h'}\right)\sum_{a=0}^{m}\sum_{b=1}^{m}\left(\frac{\frac{h'}{s}}{\sqrt{a^2+b^2}}\right)\right.\right.$$
$$-\frac{21}{25}\left(\frac{h'}{H}\right)\left(\frac{R}{H}\right)\left(\frac{R}{h'}\right)\sum_{a=0}^{m}\sum_{b=1}^{m}\left(\frac{\left(\frac{h'}{s}\right)}{\sqrt{(a^2+b^2)+\left(\frac{2h'}{s}\right)^2}}\right)$$
$$+\frac{6}{5}\left(\frac{h'}{H}\right)\left(\frac{R}{h'}\right)\sum_{a=0}^{m}\sum_{b=1}^{m}\left(\frac{\frac{h'}{s}}{\sqrt{a^2+b^2}}\right)$$
$$-\frac{6}{5}\left(\frac{h'}{H}\right)\left(\frac{R}{h'}\right)\sum_{a=0}^{m}\sum_{b=1}^{m}\left(\frac{\left(\frac{h'}{s}\right)}{\sqrt{(a^2+b^2)+\left(\frac{2h'}{s}\right)^2}}\right)$$
$$+\frac{6}{5}\left(\frac{h'}{H}\right)\left(\frac{R}{H}\right)\left(\frac{R}{h'}\right)\sum_{a=0}^{m}\sum_{b=1}^{m}\left(\frac{\left(\frac{h'}{s}\right)}{\sqrt{(a^2+b^2)+\left(\frac{2h'}{s}\right)^2}}\right)$$
$$-\frac{6}{5}\left(\frac{h'}{H}\right)\left(\frac{R}{H}\right)\left(\frac{R}{h'}\right)\sum_{a=0}^{m}\sum_{b=1}^{m}\left(\frac{\frac{h'}{s}}{\sqrt{a^2+b^2}}\right)$$
$$+\frac{18}{25}\left(\frac{R}{H}\right)\left(\frac{R}{h'}\right)\sum_{a=0}^{m}\sum_{b=1}^{m}\left(\frac{\frac{h'}{s}}{\sqrt{a^2+b^2}}\right)$$
$$\left.\left.-\frac{18}{25}\left(\frac{R}{H}\right)\left(\frac{R}{h'}\right)\sum_{a=0}^{m}\sum_{b=1}^{m}\left(\frac{\left(\frac{h'}{s}\right)}{\sqrt{(a^2+b^2)+\left(\frac{2h'}{s}\right)^2}}\right)\right]\right\} \quad (14)$$

where m is a large integer.

CHAPTER 4: RESULT AND DISCUSSION

The thesis presents the theoretical modelling for the calculation of field enhancement factor of CNTs having conical tip under any positional distribution. In the present investigation we study the variation of field enhancement factor with the angle of the conical tip. Using equation (5) we have calculated the field enhancement factor the CNTs having different opening angle varying from 15° to 45°(30° cone to 90°cone).

Variation of β_0 with angle of the conical tip:

h' (Height of the CNT) =1×10^{-6}m

$$\beta_0 = -\left\{2\left(\frac{h'}{H}\right) - \frac{3}{5}\left(\frac{h'}{H}\right)\left(\frac{R}{H}\right) - \frac{9}{50}\left(\frac{R}{H}\right)^2 + \frac{3}{5}\left(\frac{R}{H}\right) + \frac{9}{50}\left(\frac{R}{H}\right)\left(\frac{R}{h'}\right) + 3\right\}$$

Table 1: Opening angle of the conical tip of the CNT and their corresponding field enhancement factor (H (height of the conical tip) =2×10^{-9}m)

Opening angle of the cone α and the corresponding value of radius of the base of the cone	Field Enhancement factor β_0 of the single CNT
$\alpha = 15\ and\ R_{15} = 0.53nm$	922.64
$\alpha = 30\ and\ R_{30} = 1.154nm$	829.54
$\alpha = 45\ and\ R_{45} = 2nm$	701.8

Table 2: Opening angle of the conical tip of the CNT and their corresponding field enhancement factor (H (height of the conical tip) =4×10^{-9}m)

Opening angle of the cone α and the corresponding value of radius of the base of the cone	Field Enhancement factor β_0 of the single CNT
$\alpha = 15\ and\ R_{15} = 1.0717nm$	462
$\alpha = 30\ and\ R_{30} = 2.309nm$	417.7
$\alpha = 45\ and\ R_{45} = 4nm$	350.9

As we can see from the above table that if we increase the value of 'H' there is a huge reduction in the field enhancement factor from the previous one but the fact that the field enhancement factor increases with the opening angle of the cone(conical tip) remains valid. The dependence of the electric amplification factor on the aspect ratio of the nanotube is calculated for

(a) CNT modelled by cylinder with flat cap [27].

(b) CNT with the conical tip (Proposed method).

(c) CNT with hemispherical tip modelled by floating sphere [26].

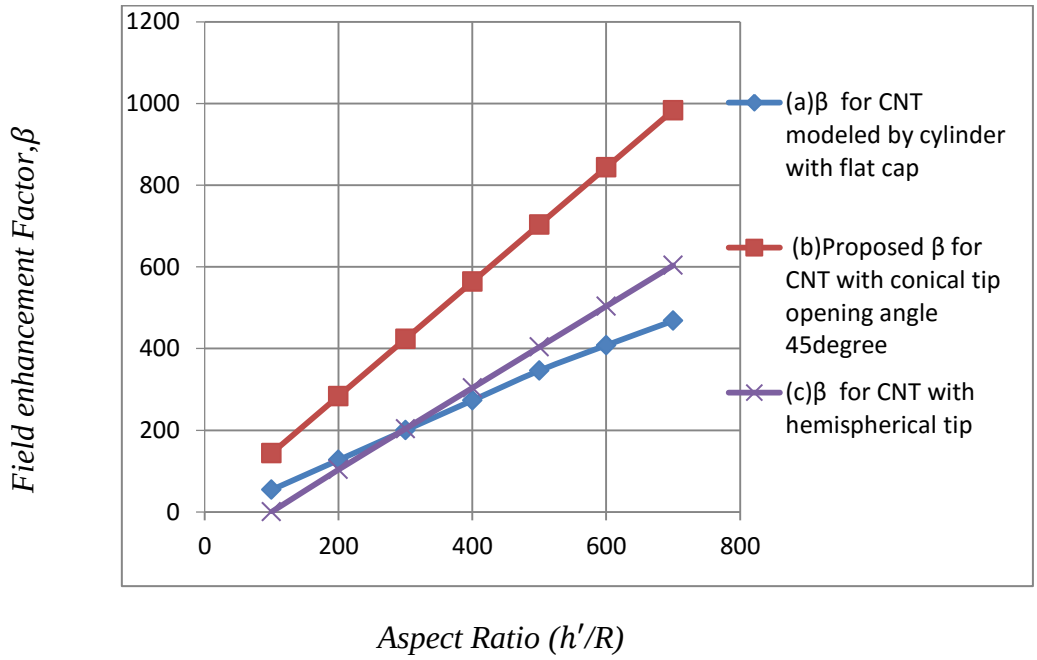

Fig 4.1: The enhancement factor for CNTs with different height and radius ratios

The above graph compares the different models for calculating the field enhancement factor and their variation with the height and radius ratio with the model proposed by us. The rhombus (a) represents nanotube that was modelled by a cylinder with a flat cap [27], the square (b) represents the proposed model which has a conical tip with 45° as opening angle and the cross (c) represents the CNTs with hemispherical tip and modelled by floating sphere model. We can see that as the (h'/R) ratio increases, the field enhancement factor is also increasing linearly. The nanotube having conical cap (opening angle 45°) can be distinguished for its high enhancement factor. However the CNT having hemispherical tip

has field enhancement factor [26] bit larger than that of the CNT modelled by cylinder with flat cap. Our result is similar to that calculated by **Eletskii** *et al*. [28]

Variation of Field Enhancement Factor taking into account the shielding effect:

$$\beta = -\left\{\beta_0 - \left[\frac{21}{25}\left(\frac{h'}{H}\right)\left(\frac{R}{H}\right)\left(\frac{R}{h'}\right)\sum_{a=0}^{m}\sum_{b=1}^{m}\left(\frac{\frac{h'}{s}}{\sqrt{a^2+b^2}}\right)\right.\right.$$
$$-\frac{21}{25}\left(\frac{h'}{H}\right)\left(\frac{R}{H}\right)\left(\frac{R}{h'}\right)\sum_{a=0}^{m}\sum_{b=1}^{m}\left(\frac{\left(\frac{h'}{s}\right)}{\sqrt{(a^2+b^2)+\left(\frac{2h'}{s}\right)^2}}\right)$$
$$+\frac{6}{5}\left(\frac{h'}{H}\right)\left(\frac{R}{h'}\right)\sum_{a=0}^{m}\sum_{b=1}^{m}\left(\frac{\frac{h'}{s}}{\sqrt{a^2+b^2}}\right)$$
$$-\frac{6}{5}\left(\frac{h'}{H}\right)\left(\frac{R}{h'}\right)\sum_{a=0}^{m}\sum_{b=1}^{m}\left(\frac{\left(\frac{h'}{s}\right)}{\sqrt{(a^2+b^2)+\left(\frac{2h'}{s}\right)^2}}\right)$$
$$+\frac{6}{5}\left(\frac{h'}{H}\right)\left(\frac{R}{H}\right)\left(\frac{R}{h'}\right)\sum_{a=0}^{m}\sum_{b=1}^{m}\left(\frac{\left(\frac{h'}{s}\right)}{\sqrt{(a^2+b^2)+\left(\frac{2h'}{s}\right)^2}}\right)$$
$$-\frac{6}{5}\left(\frac{h'}{H}\right)\left(\frac{R}{H}\right)\left(\frac{R}{h'}\right)\sum_{a=0}^{m}\sum_{b=1}^{m}\left(\frac{\frac{h'}{s}}{\sqrt{a^2+b^2}}\right)+\frac{18}{25}\left(\frac{R}{H}\right)\left(\frac{R}{h'}\right)\sum_{a=0}^{m}\sum_{b=1}^{m}\left(\frac{\frac{h'}{s}}{\sqrt{a^2+b^2}}\right)$$
$$\left.\left.-\frac{18}{25}\left(\frac{R}{H}\right)\left(\frac{R}{h'}\right)\sum_{a=0}^{m}\sum_{b=1}^{m}\left(\frac{\left(\frac{h'}{s}\right)}{\sqrt{(a^2+b^2)+\left(\frac{2h'}{s}\right)^2}}\right)\right]\right\}$$

The expression suggests the variation of field enhancement factor with length of the CNT and the spacing between the CNTs. We can take into account the effect of screening when the CNTs are distributed non -uniformly as the position of the other CNTs are taken w.r.t the CNT under consideration.

Variation of field enhancement factor with spacing between the CNTs:

On plotting field enhancement factor with respect to spacing (s) for various opening angle of the conical tip in MATHEMATICA 7 we get the following graphs;

(a)For $\alpha = 15^{\circ}$ on varying s (distance between the CNTs)(H=2nm and R=0.53nm)

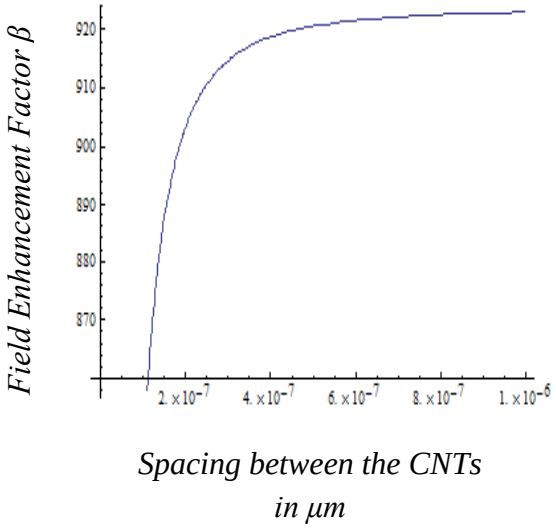

(b)For $\alpha = 30^{\circ}$ on varying s (distance between the CNTs) (H=2nm and R=1.154nm)

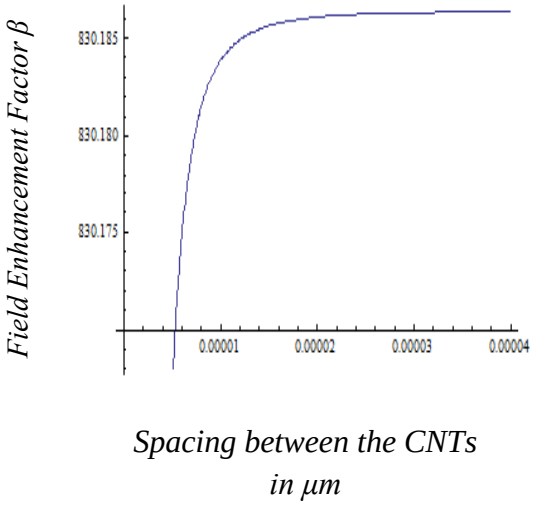

(c)For $\alpha = 45^{\circ}$ on varying s (distance between the CNTs) (H=2nm and R=2nm)

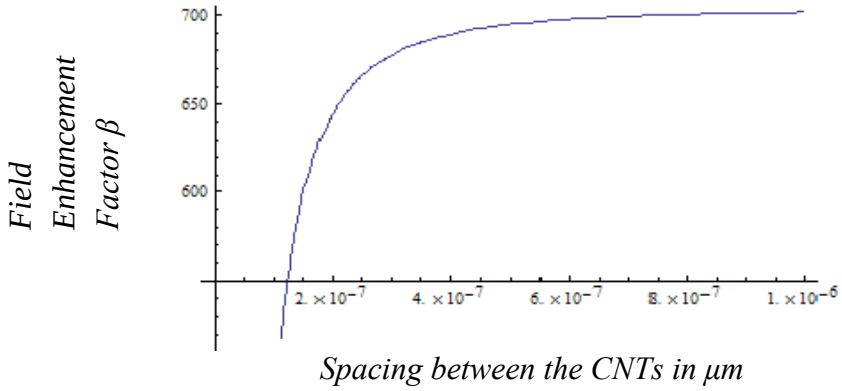

Fig 4.2: Field enhancement factor of CNTs of length 1μm and various opening angle.

Variation of field enhancement factor with length of the CNTs:

(a)For $\alpha = 15^{\circ}$ on varying h'(length of the CNTs) (H=7nm and R=1.23nm)

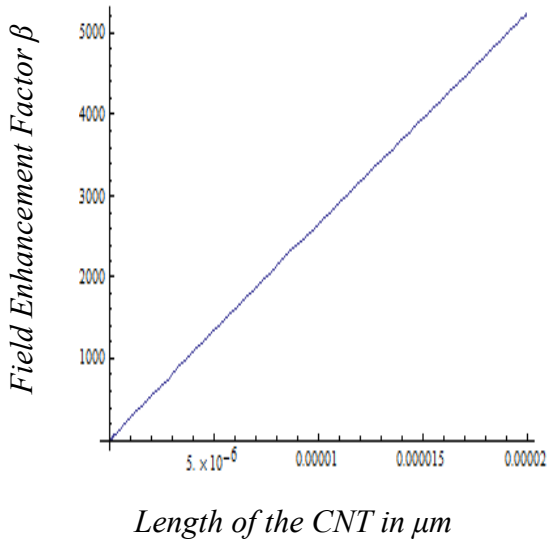

(b) For $\alpha = 30^{\circ}$ on varying h' (length of the CNTs) (H=7nm and R=4.04nm)

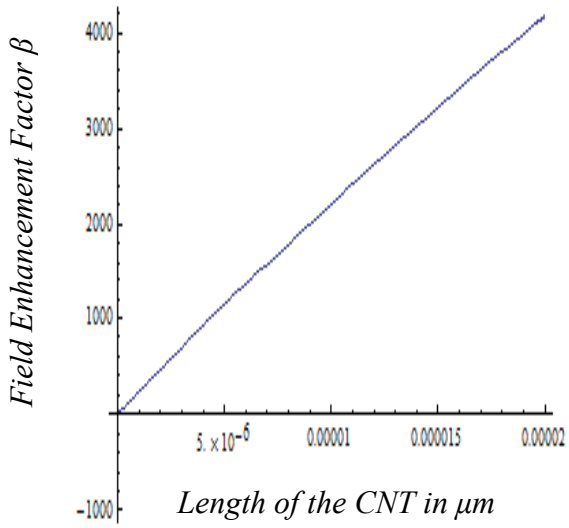

(c) For $\alpha = 45^{\circ}$ on varying h' (length of the CNTs) (H=7nm and R=7nm)

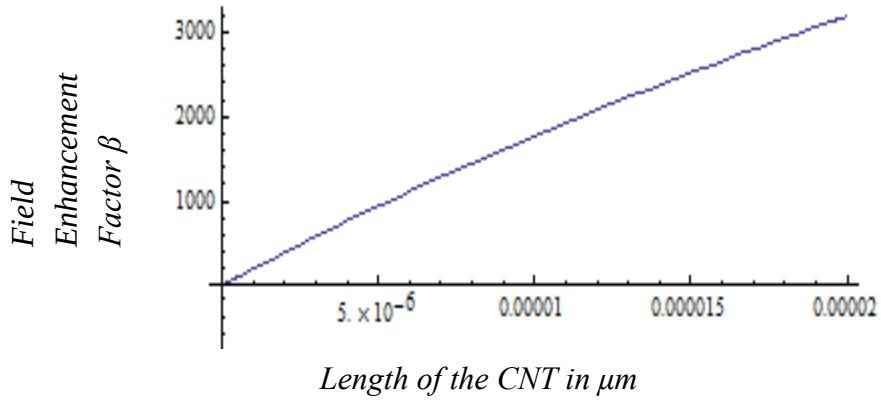

Fig 4.3: Variation of field enhancement factor with the length of the CNTs different opening angle

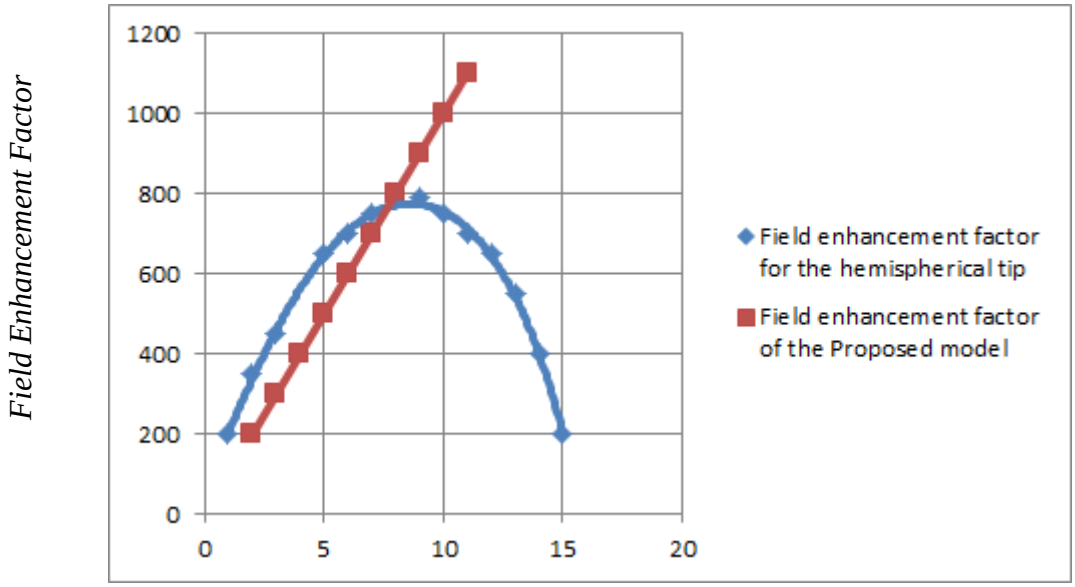

Fig4.4 Variation of field enhancement factor with length

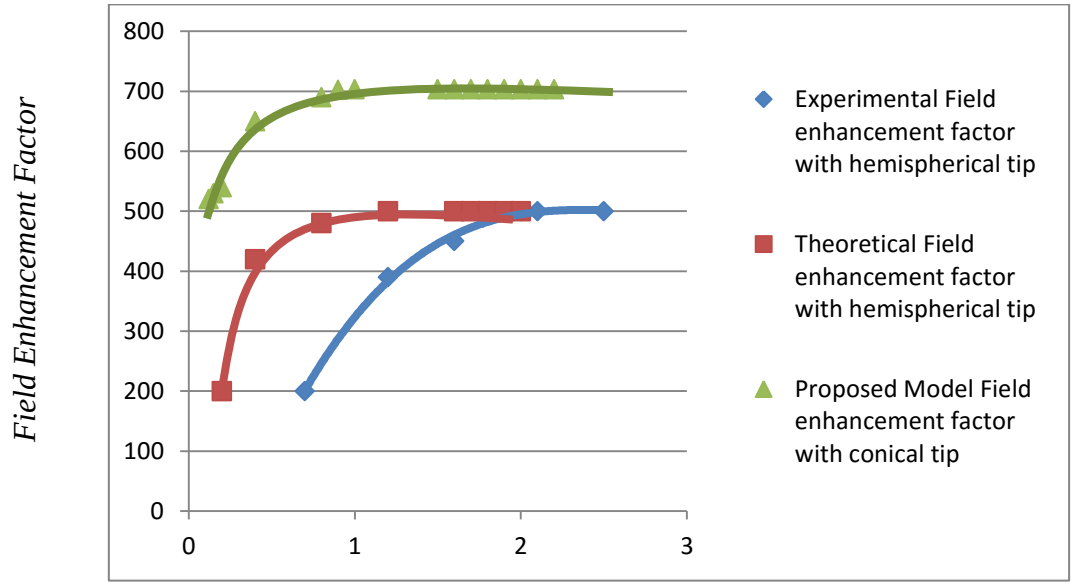

Fig 4.5 Variation of field enhancement factor with the spacing considering length of the CNT 1μm and radius 2nm.The square ones represent experimental results with hemispherical tip [29], the rhombus represents the theoretical results with hemispherical tip[26] and the triangle represents the proposed model with conical tip.

The above graphs gives us the comparison between the experimental results **Nilson** *et al.*[29], model proposed by **Ahmad** *et al.*[26] having hemispherical tip with that of our proposed having conical tip. The result which we are getting is similar with both the theoretical and experimental results. From the graph it is clear that as we increase the distance between the CNTs the field enhancement factor is increasing which is due to the reduction in shielding effect and after reaching a certain point the graph is getting saturated indicating no more shielding after a certain distance. We can see from the graphs that for the conical tip model the field enhancement factor is higher than both the experimental and theoretical results of the hemispherical tip.

CHAPTER 5: CONCLUSION

A method to compute the field enhancement factor of CNTs having any positional distribution was derived taking into account the image force. We have considered the CNTs to have a conical tip.CNTs are considered as one of the promising electron field emitters and for good field emission the tip of the CNTs plays an important role. As we can see from our results and comparing with that of the hemispherical tip, CNTs having conical tip exhibits better field emission properties. Along with the aspect ratio, the sharpness of the tip plays an important role in field emission. As the steepness of the tip increases there is an increase in the field enhancement factor. Our results are quantitatively similar to the theoretical [26, 27, 28] and experimental results [29].

REFERENCES:

[1] J.-M. Bonard, J.-P. Salvetat, T. Stöckli, L. Forro, A. Châtelain Appl. Phys. A 69, 245–254 (1999).

[2] Saito, Y.; Uemura, S.,Field emission from carbon nanotubes and its application to electron sources. Carbon 2000, 38, 169– 182.

[3] N. S. Lee , D. S. Chung , I. T. Han , J. H. Kang , Y. S. Choi , H. Y. Kim , S. H. Park , Y. W. Jin , W. K. Yi , M. J. Yun , J. E. Jung ,C. J. Lee , J. H. You, S. H. Jo , C. G. Lee , J. M. Kim, Diamond Relat. Mater.2001, **10**, 265.

[4] Jong Min Kim , Won Bong Choi, Nae Sung Lee, Jae Eun Jung, Diamond and Related Materials 9 (2000) 1184–1189.

[5] Yuan Cheng, Otto Zhou C. R. Physique 4 (2003) 1021–1033.

[6] R.H. Baughman, A.A. Zakhidov, W.A. de Heer, Science 297, 787 (2002).

[7] Yan Chen, David T. Shaw, and Liping Guo, Applied Physics Letters **76**, 2469 (2000)

[8] Gang Zhou, Wenhui Duan, and Binglin Gu Volume 87, Number 9, 095504(2001)

[9] Sanjay K. Srivastava , V. D. Vankar , Vikram Kumar , V. N. Singh, Nanoscale Res Lett (2008) 3,205–212.

[10] R. C. Smith, J. D. Carey, R. D. Forrest, and S. R. P. Silva, Journal of Vacuum Science & Technology B **23**, 632 (2005).

[11] M. S. Wang, J. Y. Wang, and L.-M. Peng Applied Physics Letters 88, 243108 (2006).

[12] Zhi Xu, X. D. Bai, and E. G. Wang, Zhong L. Wang, Applied Physics Letters 87, 163106 (2005).

[13] Seon Mi Yoon, Joseok Chae, and Jung Sang Suh Applied Physics Letters Volume 84 825 (2004).

[14] W. Zhua Bell,Bower and O. Zhou, G. Kochanski and S. Jin Applied Physics Letters **75**, 873 (1999).

[15] Jihua Zhang , Xi Wang , Wenwei Yang , Weidong Yu , Tao Feng , Qiong Li , Xianghuai Liu , Chuanren Yang Carbon 44 (2006) 418–422

[16] T. J. Vink, M. Gillies, J. C. Kriege, and H. W. J. J. van de Laar Applied Physics Letters,Volume 83 Number 17, 3552 (2003).

[17] L. H. Chan, K. H. Hong, D. Q. Xiao, W. J. Hsieh, S. H. Lai, and H. C. Shiha,T. C. Lin and F. S. Shieu K. J. Chen and H. C. Cheng Applied Physics Letter Volume 84 Number 24, 4334 (2003).

[18] Joshua M. Green, Lifeng Dong, Timothy Gutu, and Jun Jiao, John F. Conley, Jr. and

Yoshi Ono Journal of Applied Physics 99, 094308 (2006)

[19] Jung Sang Suh,Kwang Seok Jeong, and Jin Seung Lee, Intaek Han Applied Physics Letters **80**, 2392 (2002).

[20] Y.M. Wong , W.P. Kang , J.L. Davidson , B.K. Choi , W. Hofmeister , J.H. Huang , Diamond and Related Materials 14 (2005) 2078–2083.

[21] S. H. Jo ,Y. Tu ,Z. P. Huang and D. L. Carnahan ,D. Z. Wang and Z. F. Ren Applied Physics Letter, Volume 82, Number 20, 3520 (2003).

[22] X. Q. Wang, M. Wang, P. M. He, Y. B. Xu and Z. H. Li Journal of Applied Physics, Volume 96 Number 11, 6752 (2004)

[23] X. Q. Wang, M. Wang, P. M. He, Y. B. Xu and Z H Li Ultramicroscopy 102(2005)181-187.

[24] X.Q. Wang, M. Wang , H.L. Ge, Q. Chen , Y.B. Xu Physica E 30 (2005) 101–106.

[25] Richard G Forbes, C.J.Edgcombe,U.Valdre Ultramicroscopy 95 (2003)57-65

[26] Amir Ahmad and V.K Tripathi, Institute of Physics Publishing ,Nanotechnology 17(2006) 3798-3801.

[27] G. C. Kokkorakis, Greece A. Modinos and J. P. XanthakisJ.Appl.Phys., Vol 91, Number 7(2002)

[28] Alexander V Eletskii and Gregory S Bocharov ,IOP, Plasma Sources Sci. Technol. 18 (2009) 034013.

[29] L. Nilsson, O. Groening, C. Emmenegger, O. Kuettel, E. Schaller, and L. Schlapbach, H. Kind, J-M. Bonard, and K. Kern Applied Physics Letter Vol 76, Number 15, 2071 (2000)

[30] Eric W. Wong ,Paul E. Sheehan,* Charles M. Lieber,Science 277, 1971 (1997)

[31] Jean-Paul Salvetat,G. Andrew D. Briggs, Jean-Marc Bonard, Revathi R. Bacsa, Andrzej J. Kulik, Thomas Stöckli, Nancy A. Burnham, and László Forró Physical Review Letters, Volume 82, Number 5, 944(1999).

[32] O. Lourie and H. D. Wagner, J. Mater. Res., Vol. 13, No. 9, 2418-2422 (1998)

[33] Min-Feng Yu,Bradley S. Files, Sivaram Arepalli,and Rodney S. Ruoff, Physical Review Letters, Volume 84, Number 24, 5552 (2000).

[34] Min-Feng Yu, Oleg Lourie, Mark J. Dyer, Katerina Moloni,Thomas F. Kelly,Rodney S .Ruoff Science Volume 287 637-640(2000)

[35] Noriaki Hamada, Shin-ichi Sawada, Atsushi Oshiyama, Phy Review Letter, Vol 68, Number 10, 1579.(1992)

[36] P.M.Ajayan, Chem Rev , 99, 1787-1799(1991)

[37] Prabhakar R. Bandaru, Journal of Nanoscience and Nanotechnology, Vol.7, 1–29, (2007).

[38] J. Hone1, M.C. Llaguno, M.J. Biercuk, A.T. Johnson, B. Batlogg, Z. Benes, J.E. Fischer Appl. Phys. A 74, 339–343 (2002).

[39] Savas Berber, Young-Kyun Kwon, and David Tománek, Phy Review Letter, Vol 84, Number 20,4613(2000).

[40] H.Kataura,Y. Kumazawa, y.Maniwa,Synthetic Material 103, 2555-2558(1999).

[41] J.M. Bonard,Lars-olaNilsson, Solid State Electronics 45,893-914(2001).

[42] Yahachi Saito, Sashiro Uemura, Carbon 40, 1715–1728, (2002).

[43] Mirco Cantoro, Stephan Hofmann,Simone Pisana, Vittorio Scardaci, Atlus Parvez, Caterina Ducati, Andrea C. Ferrari, Arthur M. Blackburn, Kai-You Wang, and John Robertson, Nanoletters, Vol 6, Number 6, 1107-1112(2006)

[44] Kenji Hata, Don N. Futaba, Kohei Mizuno, Tatsunori Namai, Motoo Yumura, Sumio Iijima,Science ,Vol 306,1362-1363 (2004).